



HAL
open science

Homozygous haplotype deficiency in Manech Tête Rouse dairy sheep revealed a nonsense variant in MMUT gene affecting newborn lamb viability

Maxime Ben Braiek, Carole Moreno-Romieux, Céline André, Jean-Michel Astruc, Philippe Bardou, Arnaud Bordes, Frédéric Debat, Francis Fidelle, Itsasne Granado Tajada, Chris Hozé, et al.

► To cite this version:

Maxime Ben Braiek, Carole Moreno-Romieux, Céline André, Jean-Michel Astruc, Philippe Bardou, et al.. Homozygous haplotype deficiency in Manech Tête Rouse dairy sheep revealed a nonsense variant in MMUT gene affecting newborn lamb viability. 2023. hal-04158620

HAL Id: hal-04158620

<https://hal.inrae.fr/hal-04158620>

Preprint submitted on 11 Jul 2023

HAL is a multi-disciplinary open access archive for the deposit and dissemination of scientific research documents, whether they are published or not. The documents may come from teaching and research institutions in France or abroad, or from public or private research centers.

L'archive ouverte pluridisciplinaire **HAL**, est destinée au dépôt et à la diffusion de documents scientifiques de niveau recherche, publiés ou non, émanant des établissements d'enseignement et de recherche français ou étrangers, des laboratoires publics ou privés.

1 **Homozygous haplotype deficiency in Manech Tête Rousse**
2 **dairy sheep revealed a nonsense variant in *MMUT* gene**
3 **affecting newborn lamb viability**

4 Maxime Ben Braiek¹, Carole Moreno-Romieux^{1§}, Céline André², Jean-Michel Astruc³,
5 Philippe Bardou⁴, Arnaud Bordes¹, Frédéric Debat¹, Francis Fidelle², Itsasne Granado–Tajada⁵,
6 Chris Hozé⁶, Florence Plisson-Petit¹, François Rivemale¹, Julien Sarry¹, Némuel Tadi¹, Florent
7 Woloszyn¹ and Stéphane Fabre^{1*}

8 ¹GenPhySE, Université de Toulouse, INRAE, ENVT, 31326 Castanet-Tolosan, France

9 ²CDEO, Quartier Ahetzia, 64130 Ordiarp, France

10 ³Institut de l'Élevage, 24 chemin de Borde-Rouge, 31321 Castanet-Tolosan, France

11 ⁴Sigenae, INRAE, 31326 Castanet-Tolosan, France

12 ⁵Department of Animal Production, NEIKER-BRTA Basque Institute of Agricultural Research
13 and Development, Agrifood Campus of Arkaute s/n, E-01080 Arkaute, Spain

14 ⁶Eliance, 149 rue de Bercy, 75595 Paris, France

15 § *in memoriam*

16 *Corresponding author

17 Email: stephane.fabre@inrae.fr (SF)

18 Maxime Ben Braiek, ORCID iD <https://orcid.org/0000-0003-4770-0867>

19 Itsasne Granado–Tajada, ORCID iD <https://orcid.org/0000-0002-6557-1467>

20 Stéphane Fabre, ORCID iD <https://orcid.org/0000-0001-7350-9500>

21 **Abstract**

22 Recessive deleterious variants are known to segregate in livestock populations as in human, and
23 some may cause lethality when homozygous. By scanning the genome of 6,845 Manech Tête
24 Rousse dairy sheep using phased 50k SNP genotypes and pedigree data, we searched for
25 deficiency in homozygous haplotype (DHH). Five Manech Tête Rousse deficient homozygous
26 haplotypes (MTRDHH1 to 5) were identified with a homozygous deficiency ranging from 84%
27 to 100%. These haplotypes are located on OAR1 (MTRDHH2 and 3), OAR10 (MTRDHH4),
28 OAR13 (MTRDHH5) and OAR20 (MTRDHH1), and have frequencies ranging from 7.8% to
29 16.6%. When comparing at-risk mating between DHH carriers to safe mating between non-
30 carriers, two DHH (MTRDHH1 and 2) showed significant effects on decreasing artificial
31 insemination success and/or increasing stillbirth rate. We particularly investigated the
32 MTRDHH1 haplotype highly increasing stillbirth rate, and we identified a single nucleotide
33 variant (SNV) inducing a premature stop codon (p.Gln409*) in the *MMUT* gene
34 (*methylmalonyl-CoA mutase*) by using a whole genome sequencing (WGS) approach. We
35 generated homozygous lambs for the *MMUT* mutation by oriented mating, and most of them
36 died within the first 24h after birth without any obvious clinical defect. RT-qPCR and western
37 blotting performed on post-mortem liver and kidney biological samples showed a decreased
38 expression of *MMUT* mRNA in the liver and absence of a full-length MMUT protein in mutated
39 homozygous lambs. In parallel, MTRDHH4 and MTRDHH5 showed partial association with
40 variants in *RXFP2* and *ASIP* genes, respectively, already known to control horned/polled and
41 coat color phenotypes in sheep, two morphological traits accounting in the MTR breed standard.
42 Further investigations are needed to identified the supposed recessive deleterious variant hosted
43 by MTRDHH2 and MTRDHH3. Anyway, an appropriate management of these
44 haplotypes/variants in the MTR dairy sheep selection program should increase the overall
45 fertility and lamb survival.

46 **Author Summary**

47 In this article, we used reverse genetics screen in ovine using large genotype data available in
48 the framework of genomic selection program in Manech Tête Rousse dairy sheep. We identified
49 five genomic regions with a highly significant deficit in homozygous animal. These regions are
50 thus supposed to host recessive deleterious mutations. In one of these genomic regions, we
51 identified a nonsense mutation in *MMUT* that alters the functioning of this essential gene of cell
52 metabolism, causing perinatal mortality of homozygous lambs. In this work, we also identified
53 other regions possibly associated with morphological appearance part of the breed standard
54 such as polledness and coat color. Increasing knowledge in these genomic regions will help the
55 future genetic management of the Manech Tête Rousse breed, particularly to reduce lamb
56 mortality.

57 **Introduction**

58 In livestock, genetic selection has largely improved production traits over the past
59 decades, but the last one has seen the emergence of new technological tools allowing to
60 implement the genomic selection that further enhanced the genetic progress [1]. The availability
61 of high-density single nucleotide polymorphism (SNP) chip and the improvement of knowledge
62 of genomes (genome assembly and gene annotations) have allowed to fine-map genomic
63 regions and identify causal variants associated with production traits [1–4]. Despite a successful
64 selection on these traits, undesired decline of fertility was observed [5]. Although the
65 environment explains a large part of performance in ruminants), genetic studies have made it
66 possible to correct this trend and improve fertility while its heritability is less than 0.05 [6–8].

67 These studies have shown Mendelian monogenic disorders as one of the causes of fertility
68 failure.

69 Nowadays two main approaches were broadly developed to identify recessive
70 deleterious variants. The first approach is a “top-down” strategy based on case-control analysis
71 performing genome-wide association [9] when biological samples from affected animals are
72 available. In this method, distinctive phenotypes between non-affected and affected animals are
73 essential. Subsequently, homozygosity mapping approach could be performed to detect
74 homozygous regions in affected animals supposed to host the causal variant, further determined
75 by whole genome sequencing (WGS) data [10,11]. In livestock, Charlier et al. [10] have used
76 this approach for the first time and successfully detected three causal variants in cattle breeds
77 located in *ATP2A1*, *SLC6A5* and *ABCA12* genes responsible for “congenital muscular dystony”
78 types 1 (OMIA 001450-9913) and 2 (OMIA 001451-9913) and “ichthyosis fetalis” (OMIA
79 002238-9913), respectively. However, this approach showed some limits when biological
80 samples and descriptive phenotypes are not available. To raise this drawback, a second
81 approach called “bottom-up” or reverse genetic screen strategy was developed to specifically
82 identify recessive lethal variants. This strategy, initially developed by VanRaden et al. [12], is
83 based on the exploitation of large number of genotyped animals easily available from genomic
84 selection datasets to detect haplotypes showing deficit in homozygous animals, with a
85 significant deviation from the Hardy-Weinberg equilibrium. Initially, this method was
86 developed to detect embryonic lethal variant but the generalization of the method can also fine-
87 map deleterious variants leading to neonatal or juvenile lethality and morphological disorders.
88 This reverse genetic screen has successfully identified numerous deficient homozygous
89 haplotypes in several species, cattle [12–27], pigs [28,29], chicken [30], turkey [31] and horses
90 [32], and the whole genome sequencing that followed has revealed the associated causative
91 variants hosted by these regions [13,14,18,19,21,24–27,33–41]. We recently, and for the first

92 time, validated this approach in sheep with the identification of 8 independent deficient
93 homozygous haplotypes in the Lacaune dairy breed [42]. Thereafter, focusing on the Lacaune
94 Deficient Homozygous Haplotype 6 (LDHH6, OMIA 002342-9940), we identified a nonsense
95 variant in *CCDC65* gene causing juvenile mortality associated with respiratory distress when
96 homozygous [43].

97 In the present work, still leveraging genomic selection data, we searched for lethal
98 variants using a reverse genetic screen in Manech Tête Rouse (MTR) dairy sheep. This breed
99 is raised in the French Basque Country and represents the second most important breed by its
100 population size (~450,000 ewes) in France [44]. Genetic variability is well controlled in MTR
101 breed with an increase by +0.4% of inbreeding per generation over 1999-2009. The effective
102 population size ranges from 110 to 200 according to the estimation methods [44–46]. As for
103 other dairy sheep breeds in France, genomic selection in MTR was implemented in 2017 [47].

104 The aim of this study was to identify deficient homozygous haplotypes by reverse
105 genetic screen using large amount of genotyping data available in MTR dairy sheep, to test the
106 hypothesis of negative impacts on fertility traits in at-risk matings, to propose relevant candidate
107 genes located in these regions that could host recessive deleterious variants. We particularly
108 focus on one region to identify the associated causal variant from WGS data and manage at-
109 risk mating between carriers to determine the associated phenotype.

110 **Results**

111 **Identification of deficient homozygous haplotypes in Manech Tête Rouse dairy sheep**

112 Using a reverse genetic screen strategy based on 5,271 genotyped animals belonging to trios,
113 we have detected 150 highly significant Homozygous Haplotype Deficiency (HHD) of 20 SNP
114 markers (listed in S1A Table). These 150 HHD were clustered to five independent regions
115 called “Manech Tête Rouse Deficient Homozygous Haplotype” (MTRDHH). Three

116 haplotypes showed a total deficit in homozygous animals (MTRDHH1, 2 and 3), whereas two
 117 haplotypes, MTRDHH4 and 5, only showed a partial deficit (84% and 91%) with 1 and 8
 118 homozygous animals genotyped while 11 and 49 were expected, respectively (Table 1, Fig 1,
 119 S1A Table). The complete description of MTRDHH SNP markers (SNP name, SNP allele and
 120 position on sheep reference genomes Oar_v3.1, Oar_Rambouillet_v1.0 and ARS-
 121 UI_Ramb_v2.0) is available in S1B Table. The different MTRDHH were located on OAR20
 122 (MTRDHH1), OAR1 (MTRDHH2 and 3), OAR10 (MTRDHH4) and OAR13 (MTRDHH5),
 123 and their length ranged from 1.1 to 4.6 Mb on Oar_rambouillet_v1.0. The observed frequencies
 124 of heterozygous carriers were between 7.8% and 16.6%. MTRDHH2 and MTRDHH3 both
 125 located on OAR1 were not in linkage disequilibrium. Consequently, the five MTRDHH
 126 identified are likely to harbor five independent variants causal of the observed homozygous
 127 deficiency.

128 **Table 1. List of Manech Tête Rouse deficient homozygous haplotypes.**

Haplotype	OAR	Number of markers	Position (Mb)	Heterozygous carrier frequency (%)	Number of homozygotes			
					Exp	Obs	Deficit (%)	Poisson P-value
MTRDHH1	20	32	23.0-25.0	9.7	13	0	100	2.9×10^{-6}
MTRDHH2	1	66	251.9-256.4	8.7	10	0	100	3.8×10^{-5}
MTRDHH3	1	39	103.8-106.6	7.8	9	0	100	9.6×10^{-5}
MTRDHH4	10	26	30.5-31.5	8.7	11	1	91	1.5×10^{-4}
MTRDHH5	13	29	64.3-67.2	16.6	49	8	84	5.3×10^{-13}

129 ^aMTRDHH haplotypes and SNP markers composition are details in S1 Table

130 ^bPosition on ovine genome assembly Oar_rambouillet_v1.0

131 ^cFrequency of carriers in the entire genotyping population (n=6,845)

132 ^dExpected

133 ^eObserved

134 **Impact of MTRDHH on fertility traits**

135 In order to identify a putative lethal effect of the five MTRDHH, two recorded fertility traits
 136 were analyzed: artificial insemination success, a proxy for embryonic loss (AIS: 330,844
 137 matings) and stillbirth rate associated with perinatal lethality (SBR: 201,637 matings) (Fig 2).
 138 The average AIS of the population was 60.9%. When comparing at-risk and safe matings, only

139 MTRDHH2 showed a significant decrease of -3.3% of AIS ($P=3.5\times 10^{-4}$) in at-risk matings.
140 The average SBR of the population was 7.5%. As described in Fig 2, MTRDHH1 and 2 showed
141 a huge increase in SBR with +7.5% ($P=4.0\times 10^{-24}$) and +4.3% ($P=1.3\times 10^{-6}$) in at-risk matings
142 compared to safe matings, respectively. The three other haplotypes showed no significant
143 impact on the fertility traits studied.

144 **Pleiotropic effects of MTRDHH on milk production traits**

145 Six dairy traits are routinely included in genomic evaluation of the French dairy sheep. Thus,
146 standardized daughter yield deviation (sDYD) of five milk production traits (milk, fat and
147 protein yields, and fat and protein contents) and lactation somatic cell score (a proxy for udder
148 health) were compared between carrier and non-carrier rams for each of the 5 MTRDHH
149 evidenced (Fig 3). Among the five haplotypes, three were associated with significant effect on
150 sDYD. Daughters of MTRDHH2 carrier rams showed a significant increase in milk production
151 (sDYD +0.06, $P=6.5\times 10^{-3}$) but a decrease in protein content (sDYD -0.11, $P=4.7\times 10^{-4}$). For
152 MTRDHH4, there was a significant increase in lactation somatic cell score (sDYD -0.13,
153 $P=2.4\times 10^{-3}$), and daughters of MTRDHH5 carrier rams showed higher fat yield (sDYD -0.06,
154 $P=9.6\times 10^{-3}$). Additionally, the total merit genomic index, named ISOLg, was extracted from
155 each male lamb of the 2021 genomic selection cohort to estimate the MTRDHH impact on the
156 genetic gain of the selected traits. No significant difference was observed on ISOLg between
157 heterozygous carrier and non-carrier lambs for each MTRDHH (S1 Fig).

158 **Evolution of the MTRDHH frequencies in the population**

159 Since the implementation of genomic selection in 2017, all candidate rams coming from elite
160 mating were genotyped on low density SNP chip at 7 days old, representing the genetic
161 diversity disseminated by AI in the selection scheme. As shown in Fig 4, the frequencies of the

162 MTRDHH heterozygous carriers were quite stable during the last five years around 6.8, 7.4,
163 9.3, 10.2 and 16.1% for MTRDHH1, 2, 3, 4 and 5, respectively. Nevertheless, we can notice a
164 spectacular increase in the frequency of MTRDHH3 from 2.8% to 10.9% when comparing 2017
165 and 2018.

166 **Candidate genes located in MTRHH regions**

167 Within the five MTRDHH genomic regions extended by 1Mb on each side, 408 protein coding
168 genes are annotated (S2 Table). When available, information on mouse phenotypes (including
169 lethal phenotypes) and association with mammalian genetic disorders were extracted for each
170 gene using MGI, IMPC, OMIM and OMIA databases. Among the 408 genes, we highlighted
171 64 genes involved in lethal phenotypes in knock-out mice, and 45 genes associated with human
172 genetic disorders. Twenty-three relevant candidate genes were identified by the intersection of
173 both information (Fig 5). In addition, 7 genes are known to be associated with genetic disorders
174 or morphological traits in livestock (*GJA5*, *ITGA10*, *ADAMTLS4*, *RXFP2*, *KIF3B*, *ASIP* and
175 *CEP250*). Overall, these candidate genes are involved in essential functions such as
176 transcription (*POLR3GL*, *SF3B4*, *PRPF3*, *ASXL1* and *DNMT3B*), cell division (*POGZ*, *BRCA2*,
177 *PIGU* and *CEP250*), basal metabolic processes (*MMUT*, *SLC33A1*, *TARS2* and *AHCY*), cell
178 structure and signaling (*CD2AP*, *PKHD1*, *GJA5*, *ITGA10*, *ECM1*, *GJA5*, *ITGA10*, *ECM1*,
179 *PRUNE1*, *RXFP2*, *KL*, *POFUT1*, *KIF3B*, *ASIP* and *GSS*), and DNA/protein binding (*TFAP2B*
180 and *PEX11B*).

181 **Known variants in *RXFP2* and *ASIP* genes are partially associated with MTRDHH4 and** 182 **MTRDHH5**

183 The above list of candidate genes particularly highlighted *RXFP2* (within MTRDHH4) and
184 *ASIP* (within MTRDHH5) genes well-known to impact sheep morphological traits such as

185 polledness [48] and black coat color [49,50], respectively. Interestingly, horned female and
186 black males are not desired in accordance with the MTR breed standards. Using the 22 WGS
187 of MTR animals, we searched for the 1.8kb insertion in the 3'-UTR of *RXFP2* associated with
188 polledness (OMIA 000483–9940, [48]) and the different variants affecting *ASIP* leading to
189 recessive black coat color (OMIA 000201-9940); OAR13:g.66,475,132_66,475,136del and
190 g.66,474,980T>A, Oar_rambouillet_v1.0) [49,50]. S2 Fig shows the segregation of these
191 variant among the 22 sequenced animals and their relationship with the status of MTRDHH4
192 and 5, but with no obvious association. This being made on a reduced number of animals, we
193 specifically genotyped a larger set of animals (n=714 male lambs born in 2021) for the 1.8kb
194 insertion in *RXFP2* and the two variants in *ASIP*. Using this cohort, we evidenced a partial
195 association between MTRDHH4 and the 1.8kb insertion in the 3'-UTR of *RXFP2*, none
196 heterozygous MTRDHH4/+ being Del/Del corresponding to the horned phenotype (Fig 6).
197 Concerning *ASIP* variants, MTRDHH5 was also partially associated with the 5pb deletion.
198 Indeed, 89% of the MTRDHH5 heterozygous carriers were heterozygous for the 5pb deletion
199 and none Ins/Ins animal was MTRDHH5 carrier. In contrast, we identified almost the same
200 proportion of genotypes for g.66,474,980T>A in MTRDHH5 carriers and non-carriers (+/+),
201 suggesting that MTRDHH5 was not linked to this polymorphism (Fig 6C).

202 **Identification of a nonsense variant in *MMUT* gene associated with MTRDHH1**

203 With the most important impact on stillbirth rate increased by +7.5% in at-risk matings (Fig 2),
204 we particularly focused on MTRDHH1 that may represent a putative recessive lethal haplotype.
205 In order to identify the MTRDHH1 causal mutation, we have considered biallelic variants (SNP
206 and InDels) for 100 ovine WGS containing the 22 Manech Tête Rousse dairy sheep, and among
207 them two heterozygous carriers of the MTRDHH1 haplotype. Within the MTRDHH1 region
208 extended by 1Mb on each side, 78,019 variants were called with a quality score >30, call rate

209 >95% and only four candidate variants had a perfect correlation ($r^2=1$) between biallelic variant
 210 genotypes and MTRDHH1 status (Table 2, Fig 7A). Among those candidate variants, we
 211 identified two small insertions, one intergenic single nucleotide variant (SNV), and one
 212 nonsense (stop-gain) SNV located in the *Methylmalonyl-CoA Mutase (MMUT)* gene. This latter
 213 SNV (NC_040271.1: g.23,776,347G>A; XM_004018875.4: c.1225C>T; Fig 7B, C) in *MMUT*
 214 is predicted to create a premature stop codon at position 409 encoded by exon 6
 215 (XP_004018923.1:p.Gln409*) whereas the full protein length is composed of 750 amino acids
 216 (Fig 7D). The variant would disrupt the methylmalonic coenzyme-A mutase domain and would
 217 result in the loss of the vitamin B12 binding domain.

218 **Table 2. Candidate variants located in MTRDHH1.**

Position	Ref/Alt	Quality score	Location Annotation	Functional Consequence ^a
23,436,234	G/GTCACA	385.8	Intergenic	Modifier
23,436,236	T/TTTGTG	385.8	Intergenic	Modifier
23,776,347	G/A	146.0	Exonic, <i>MMUT</i> (c.1225C>T)	High, stop-gain (p.Gln409*)
23,969,676	C/T	370.3	Intergenic	Modifier

219 ^aVariant annotation and effect predicted by SnpEff [51].

220 In order to validate the association between the *MMUT* variant and MTRDHH1, we
 221 genotyped the cohort of male lambs born in 2021 (n=714) with a specific genotyping test for
 222 the *MMUT* g.23,776,347G>A SNV. The A variant allele frequency was 3.8%. All these animals
 223 have a known status at the MTRDHH1 locus and the contingency table indicates a clear
 224 association between the MTRDHH1 status and *MMUT* variant genotypes (Fig 8, Fischer's exact
 225 test $p<0.0001$). However, 15 animals showed discrepancy between *MMUT* and MTRDHH1
 226 genotypes, supposed to be in perfect linkage disequilibrium. A specific focus on haplotypes
 227 carried by these animals in the MTRDHH1 region from marker 1 (s75212.1) to marker 32
 228 (OAR20_24583511.1) showed that the 14 animals heterozygous for the variant exhibited
 229 shorter recombinant versions of the MTRDHH1 haplotype (S3 Fig). Nonetheless, one animal

230 was heterozygous for MTRDHH1 but did not carry the *MMUT* variant.

231 **Occurrence of the *MMUT* SNV in an ovine diversity panel**

232 An ovine diversity panel composed of 25 French sheep breeds, including MTR, and 3 Latxa
 233 Spanish sheep breeds related to MTR was used to genotype the *MMUT* g.23,776,347G>A SNV
 234 (Table 3). As expected, some MTR animals (n=5) from this panel were evidenced as
 235 heterozygous carriers, and the variant was also detected in one animal of the Spanish Latxa
 236 Cara Rubia population. All the other animals tested did not carry the polymorphism.

237 **Table 3. *MMUT* SNV genotype distribution from a DNA diversity panel of French (FR)
 238 and Spanish (ES) ovine breeds.**

Breed	Total	Genotype		Breed	Total	Genotype	
		G/G	A/G			G/G	A/G
Berrichon du Cher (FR)	30	30		Martinik (FR)	23	23	
Blanche du Massif Central (FR)	31	31		Merinos d'Arles (FR)	27	27	
Causse du Lot (FR)	32	32		Mourerous (FR)	26	26	
Charmoise (FR)	31	31		Mouton Vendéen (FR)	30	30	
Charollais (FR)	30	30		Noir du Velay (FR)	28	28	
Corse (FR)	30	30		Préalpes du sud (FR)	27	27	
Ile de France (FR)	28	28		Rava (FR)	29	29	
Lacaune (Meat) (FR)	45	45		Romane (FR)	30	30	
Lacaune (Milk) (FR)	40	40		Romanov (FR)	26	26	
Latxa Cara Negra Euskadi (ES)	30	30		Rouge de l'Ouest (FR)	30	30	
Latxa Cara Negra Navarra (ES)	40	40		Roussin (FR)	30	30	
Latxa Cara Rubia (ES)	30	29	1	Suffolk (FR)	29	29	
Limousine (FR)	30	30		Tarasconnaise (FR)	33	33	
Manech Tête Rousse (FR)	29	24	5	Texel (FR)	27	27	
				Total	851	845	6

239 **Viability of homozygous lambs for the *MMUT* variant**

240 To validate the impact of the *MMUT* A variant allele we have manage an oriented mating
 241 between heterozygous carriers to generate homozygous lambs. Blood samples were collected
 242 from 181 MTR ewes, daughters of MTRDHH1 carrier sires, in 6 private farms. The *MMUT*
 243 SNV specific genotyping identified 82 heterozygous ewes. Among these ewes, 73 were raised

244 in the 6 private farms (Experiment 1) and 9 were moved into an INRAE experimental farm
245 (Experiment 2). All ewes were artificially inseminated with fresh semen from *MMUT*
246 g.23776347G/A heterozygous rams. Forty-five days after AI, 44 and 5 were diagnosed as
247 pregnant by ultrasonography in Experiment 1 and 2, respectively. This corresponds to an AIS
248 of 59.8% in accordance with the average AIS of 60.9% determined previously in the whole
249 population. In experiment 1, only 37 among the 44 pregnant ewes were monitored after
250 gestation diagnosis and resulted in the birth of 59 lambs (mean prolificacy of 1.6, litter size
251 ranging from 1 to 3) with a gestation length between 139 and 159 days. In experiment 2, the 5
252 pregnant ewes gave birth to 13 lambs (mean prolificacy of 2.6, litter size ranging from 2 to 4)
253 with a gestation length between 151 and 157 days. No abortion during the five months of
254 gestation was observed. Finally, 72 lambs (52% males and 48% females) were born and an ear
255 punch was collected for genotyping the *MMUT* SNV (Table 4). The distribution of genotypes
256 did not differ between the two experiments (Fisher's exact test, $p=0.686$). In total, 21 lambs
257 were genotyped homozygous carriers (A/A), 29 heterozygous carriers (A/G) and 21
258 homozygous non-carriers (G/G). All lambs were monitored during the 0-30 days period until
259 weaning. Twenty-five lambs died during this period representing a huge mortality rate of 34.7%
260 (Fig 9). Contingency table between lamb genotypes (A/A, G/A, G/G) and viability (alive or
261 dead) indicated a higher mortality rate for homozygous A/A lambs (Table 4, Fisher's exact test,
262 $p<0.001$). Indeed, the A/A dead lambs accounted for 78% of the whole lamb mortality. The
263 death of A/A homozygous lambs occurred very soon after birth within the first 24 hours.
264 Clinical examination of dead lambs did not allow us to identify specific symptoms. Two
265 homozygous A/A lambs have passed the weaning age (around 4 weeks). Additionally, in
266 Experiment 2, the 13 lambs were weighted at birth (males: 4.0 ± 0.9 kg, females: 2.9 ± 1.4 kg)
267 and A/A lambs had significantly lower birth weight compared to the other genotypes, regardless
268 gender (Wilcoxon's non parametric test, $p=0.019$) (Fig 10).

269 **Table 4. Genotyping results of lambs generated in at-risk matings in private and**
 270 **experimental farms according to the sex and *MMUT* SNV genotype.**

	g.23,776,347G>A genotype in <i>MMUT</i>				Total
	G/G	G/A	A/A	-/-	
<u>Experiment 1:</u>					
Private farms (n=6)					
Male	9	9	10	1	29
Female	8	16	5		29
Undetermined			1		1
Total	17	25	16	1	59
<u>Experiment 2:</u>					
Experimental farm (n=1)					
Male	4	2	2		8
Female	0	2	3		5
Total	4	4	5		13
<u>All</u>					
Male	13	11	12	1	37
Female	8	18	8	0	34
Undetermined			1		1
Total	21 (19^a/2[†])	29 (25^a/4[†])	21 (2^a/19[†])	1* (0^a/1[†])	72

271 *The ear punch was not available for this lamb.

272 ^a Number of alive lambs.

273 [†] Number of dead lambs.

274 **MMUT protein expression and activity**

275 Based on the sheep gene atlas (<http://biogps.org/sheepatlas/>; accessed 17 February
 276 2022), *MMUT* is shown to be highly expressed in kidney and liver [52]. In order to evidence a
 277 putative nonsense-mediated mRNA decay (NMD) due to the nonsense variant in *MMUT*, we
 278 evaluated the *MMUT* mRNA relative expression in kidney and liver by qPCR (Fig 11A). We
 279 evidenced a significant reduction of *MMUT* expression in liver (Wilcoxon's non parametric
 280 test, p=0.0015) but not in kidney (Wilcoxon's non-parametric test, p=0.66). We also assessed
 281 the *MMUT* protein expression from liver and kidney protein extracts collected from two
 282 homozygous A/A and two homozygous G/G dead lambs. As expected, using Western blotting,
 283 the wild type protein was expressed in kidney and liver whereas the mutated protein was not

284 detected at least as a full-length form in both tissues (Fig 11B). We also tried to evaluate the
285 accumulation of methylmalonic acid quantified by ELISA in urine and blood of A/A lambs
286 collected post-mortem or soon after birth in alive animals (Fig 12) but no significant difference
287 was observed compared to G/G or G/A lambs (Wilcoxon's non-parametric test, $p=0.54$ in urine,
288 Wilcoxon's non-parametric test, $p=0.34$ in plasma).

289 Discussion

290 Using a reverse genetic screen in MTR population, we successfully identified five genomic
291 regions (named MTRDHH1 to 5) with a significant deficit of homozygous animals ranging
292 from 84 to 100%. Compared to our previous analysis in Lacaune dairy sheep with 8 independent
293 haplotypes, we identified less deficient haplotypes in MTR possibly due to a lower number of
294 genotyped animals (19,102 Lacaune vs 6,845 MTR) [42]. In the MTR population, we estimated
295 the frequencies of MTRDHH heterozygous carriers between 7.8% and 16.6%, and thus allele
296 frequency between 3.9 and 8.3%. This is in line with an allele frequency of 5% expected from
297 the analysis of a population of 6,000 genotyped animals [24].

298 We tested a putative impact of each MTRDHH on production traits to search for a selective
299 advantage at heterozygous state. The positive effects of these DHH on selected traits were quite
300 low and only significant for MTRDHH2 carriers on milk yield and for MTRDHH5 on fat yield.
301 It is thus unlikely that selective advantage explains the observed DHH frequencies, or the rapid
302 increase in MTRDHH3 frequency between 2017 and 2018. However, many examples of
303 balancing selection for deleterious alleles have been described in livestock [53]. For example
304 in sheep, a missense variant in *FGFR3* was associated with enhanced skeletal growth and meat
305 yield when heterozygous while it induced chondrodysplasia (spider lamb syndrome) when
306 homozygous (OMIA 001703-9940) [54].

307 The populational analysis of AIS and SBR recorded on more than 300,000 matings, allowed
308 us to do a first sorting of the different MTRDHH based on their supposed deleterious impact
309 on early gestation (AIS), around the time of birth (SBR), or on postnatal viability or
310 morphological phenotypes when AIS and SBR were not altered. Accordingly, we classified the
311 five haplotypes into three groups and we highlighted potential candidate genes according to
312 their implication in lethal phenotypes in mouse and/or more generally involved in inherited
313 mammalian disorders.

314 The first group is composed of MTRDHH3 (OAR1), MTRDHH4 (OAR10) and
315 MTRDHH5 (OAR13) which showed no significant impact on fertility traits. We assume that
316 these haplotypes host deleterious variants leading to postnatal lethality or morphological
317 disorders. Within these three regions, 18 candidate genes are of interest for their implication in
318 neonatal to juvenile lethality or associated with morphological defects counter selected at the
319 time of candidate lamb genotyping. Candidate genes associated with postnatal lethality mainly
320 affect metabolism (*TARS2* in MTRDHH3, *KL* in MTRDHH4) or DNA repair (*BRCA2* in
321 MTRDHH4). Some candidate genes not necessarily lead to lethality when altered, but may
322 affect animal welfare with the alteration of vision (*PRPF3*, *ADAMTSL4* in MTRDHH3 and
323 *KIF3B* in MTRDHH5), neurological disorders (*PRUNE1*, *POGZ* in MTRDHH3 and *ASXLI*,
324 *PIGU*, *AHCY* in MTRDHH5) or morphological/stature defects (*ITGA10*, *POLR3GL*, *ECM1* in
325 MTRDHH2 and *DNMT3B*, *CEP250* in MTRDHH5). However, by searching causal variants in
326 the 22 WGS of MTR animals, we failed to detect candidate mutations in the genes listed above.
327 In contrast, we were puzzled by the presence of *RXFP2* (MTRDHH4) and *ASIP* (MTRDHH5)
328 as positional candidate genes already known to host variants controlling the horned/polled
329 phenotype (OMIA 000483–9940) [48] and black coat color (OMIA 000201–9940) [49,50] in
330 sheep, respectively. Interestingly, in MTR selection scheme, horned females and black animals
331 do not fit with breed standard, and thus are not desirable. This may lead excluding these animals

332 from genotyping which fully express their phenotype at the homozygous state. Accordingly,
333 based on specific SNP markers already present on the LD SNP chip used, we were able to
334 significantly associate MTRDHH5 with the 5pb deletion in *ASIP* leading to black coat color
335 when homozygous. In contrast, the deficit observed for MTRDHH4 is significantly associated
336 with the Ins allele of *RXFP2* leading to the desirable polledness trait. This intriguing
337 observation suggests a hitchhiking phenomenon explaining the deficit [55], with the presence
338 of a deleterious variant in linkage disequilibrium with the Ins allele of *RXFP2*.

339 The second group with MTRDHH2 (OAR1) associated with significant negative effects on
340 AIS and SBR. Then, we hypothesized that the causative variant hosted by MTRDHH2 could
341 induce embryo/fetal losses throughout the gestation period and until birth. In this region, only
342 *SLC33A1* (*Solute Carrier Family 33 Member 1*) gene has both impact on embryonic lethality
343 and decrease survival rate when knocked-out in mouse (MGI:1332247) and thus appears as an
344 obvious candidate gene. In addition, variants in *SLC33A1* (OMIM 603690) are known to cause
345 “Congenital cataracts, hearing loss, and neurodegeneration” and “Spastic paraplegia 42”
346 phenotypes [56,57]. A study is ongoing to evidence a candidate causal variant affecting the
347 *SLC33A1* gene in linkage disequilibrium with MTRDHH2.

348 MTRDHH1 (OAR20) was the only haplotype with a strong negative impact exclusively on
349 SBR suggesting that this haplotype hosts a lethal variant affecting the perinatal period. Within
350 the MTRDHH1 region, we identified *MMUT* (*Methylmalonyl-CoA Mutase*), *TFAP2B*
351 (*Transcription Factor AP-2 Beta*) and *PKHD1* (*PKHD1 Ciliary IPT Domain Containing*
352 *Fibrocystin/Polyductin*) as obvious candidate genes, all resulting in neonatal and/or postnatal
353 lethality when knocked-out in mouse. *MMUT* and *PKHD1* are involved in metabolic disorders
354 such as “Methylmalonic aciduria” (OMIM 251000) and “Polycystic kidney disease” (OMIM
355 263200), respectively. *TFAP2B* is involved in bone defects and heart failure (OMIM 169100).
356 Using WGS data from 22 MTR animals and among them, two MTRDHH1 heterozygous

357 carriers, we were able to identify four candidate polymorphisms within MTRDHH1, but only
358 one appeared as a strong functional candidate, a SNV (G>A) located in the *MMUT* gene at
359 position g.23,776,347 on OAR20. This SNV leads to a nonsense variation XM_004018875.4:
360 c.1225C>T introducing a premature stop-codon (p.Gln409*). The genotyping of
361 g.23,776,347G>A in 714 animals with a known status at MTRDHH1 indicated an almost
362 perfect association. The only 15 discordant animals were largely explained by shorter
363 recombinant version of the MTRDHH1 haplotype (between 2 to 31 markers surrounding the
364 SNV). Only one MTRDHH1 heterozygous carrier did not carry the *MMUT* variant. This
365 discrepancy could be attributed to errors from SNP array genotyping, phasing and/or
366 imputation. Immunoblotting realized on liver and kidney proteins extracts from homozygous
367 carrier lambs has confirmed the predicted impact of the candidate SNV on the protein. The anti-
368 *MMUT* antibody has revealed a band at 83kDa as expected for the full-length *MMUT*
369 polypeptide in wild-type extract. In contrast, due to the lack of the antigenic epitope (from aa
370 451 to 750) in the p.Gln409* truncated form, the *MMUT* band was not detected in homozygous
371 carriers proving that this SNV has an effect on the functional expression of the *MMUT* gene,
372 reinforced by a NMD phenomenon detected in liver. In order to confirm the perinatal lethality
373 supposed for MTRDHH1 increasing SBR by 7.5%, we have managed at-risk mating between
374 heterozygous carriers of the p.Gln409* variant. In this experiment, 84% of homozygous lambs
375 died within the first 24 hours after birth fitting perfectly with the hypothesis and explaining the
376 complete deficit of homozygous carriers of MTRDHH1 in the DHH analysis, due to lethality
377 before the time of genotyping. We also evidenced that homozygous newborn lambs had a lower
378 birth weight, an observation which could be compared to postnatal growth retardation in *Mmut*
379 knock-out mice (MGI:5527455).

380 In human, numerous pathogenic variants in *MMUT* cause “Methylmalonic aciduria”
381 (OMIM 609058, MMA, [58]), an autosomal recessive metabolism disorder. *MMUT* is part of

382 a metabolic pathway starting from the degradation of amino acids (Valine, Isoleucine,
383 Methionine and Threonine), odd-chain fatty acids, cholesterol and propionic acid to succinyl-
384 CoA by three main enzymes: Propionyl-CoA carboxylase (PCC), Methylmalonyl-CoA
385 epimerase (MCE) and Methylmalonyl-CoA mutase (MMUT) [59,60]. The MMUT protein is a
386 mitochondrial enzyme that catalyze the L-methylmalonyl-CoA to succinyl-CoA, an
387 intermediate of Krebs cycle. The isomerization of methylmalonyl-CoA requires
388 adenosylcobalamin (AdoCbl), the cofactor form of vitamin B12 (also known as Cobalamin)
389 [61]. In sheep, the mutant protein (p.409Gln*) does not carry the B12 binding domain (615-733
390 amino acids), suggesting that the AdoCbl cofactor is unable to act in the conversion of L-
391 methylmalonyl-CoA to succinyl-CoA. When the MMUT enzyme is not functional,
392 methylmalonic acid (MLA) accumulates in body fluids, mainly in blood and urine [60,62].
393 However, we failed in evidencing such MLA accumulation in plasma or urine of homozygous
394 A/A lambs, while this was observed in homozygous knock-out mouse 24h after birth [63]. In
395 our study, many of our urine and blood samples were collected at necropsy only after natural
396 death of the lambs without time control, possibly affecting the results. The methylmalonic
397 aciduria in this sheep genetic model will need further clinical investigation.

398 All the above elements clearly indicate that the deficit of homozygous MTRDHH1 is due
399 to a loss-of-function mutation in the *MMUT* gene altering an essential metabolic pathway.
400 Many reverse genetic screen approaches have also evidenced the association of DHH with
401 mutations in genes implied in metabolism [64]. Particularly in bovine, many variants were
402 evidenced affecting metabolic processes in several breeds such as Braunvieh (BH24/*CPT1C*,
403 lipid metabolism) [19], Holstein (HH4/*GART*, nucleotide metabolism) [13], Montbéliarde
404 (MH1/*PFAS*, nucleotide metabolism ; MH2/*SLC37A2*, glucose metabolism) [13,40],
405 Normande (NH7/*CAD*, nucleotide metabolism) [26], and Simmental (SH8/*CYP2B6*, respiratory
406 chain) [27].

407 Diversity analysis have also revealed the segregation of *MMUT* SNV variant in Spanish
408 Latxa Cara Rubia (LCR) breed. French MTR and Spanish LCR are very close populations.
409 Since 1970s, many exchanges have occurred between these population across the border, first
410 from Spain to France during the seventies, then the reverse since the nineties [65]. The *MMUT*
411 SNV evidenced in this study is not shared by other French sheep breeds and more largely by
412 the individuals from the International Sheep Genome Consortium (dataset composed of 453
413 animals from 38 breeds all over the world, <https://www.sheephapmap.org/>). However,
414 searching this dataset, we found another SNV located in ovine *MMUT* gene (rs1093255812)
415 leading to a premature stop-gain (ENSOART00020022357.1: p.Trp43*). This variant was
416 identified at heterozygous state in the New Zealand Coopworth breed, and as in MTR, it could
417 have the same deleterious impact on lamb viability.

418 **Conclusion**

419 In this study, we firstly identified in the MTR dairy sheep the segregation of five
420 independent haplotypes possibly hosting five recessive deleterious alleles of which at least three
421 have negative impact on fertility traits. Among them, we evidenced the *MMUT* c.1225T
422 (p.409Gln*) variant associated with the MTRDHH1 haplotype causing early lamb mortality
423 when homozygous. This could provide an excellent animal model for the study of
424 methylmalonic aciduria occurring in human with the same recessive genetic determinism
425 affecting *MMUT*. The MTRDHH2 and 3 represent promising haplotypes to discover other
426 recessive lethal mutations in the near future. This reverse genetic study has also allowed us to
427 hypothesize that two of these haplotypes, MTRDHH4 and 5, do not associate with lethal
428 mutations but with mutations possible affecting morphological traits. The causal mutations are
429 still to be identified since the already known mutations in *RXFP2* and *ASIP* do not fit perfectly

430 with the segregation of these two haplotypes. Anyway, an appropriate management of these
431 haplotypes/variants in the MTR dairy sheep selection program should increase the overall
432 fertility and lamb survival, and may help for selection of morphological breed standards.

433 **Materials and methods**

434 **Animal and genotyping data**

435 The total dataset is composed of 6,845 genotyped Manech Tête Rousse animals (82% males
436 and 18% females) born between 1993 and 2021 (data description in S4 Fig). Genotyping was
437 performed at the Labogena facility (<http://www.labogena.fr/>) in the framework of the French
438 dairy sheep genomic selection [66]. Both low density 15k SNP chip (SheepLD; n=2,956) and
439 medium density 50k SNP chip (Ovine SNP50 BeadChip; n=3,889) were purchased from
440 Illumina Inc. (San Diego, USA) (Table 5). Pedigree information was extracted from the official
441 national database SIEOL (*Système d'Information en Elevage Ovin Laitier*, France).

442 **Table 5. Description of genotyped animals**

Year of birth	< 2017	≥ 2017		Total
Background	Research programs	Genomic selection & Research programs		
Number of animals	2,533 rams	3,077 rams		6,845
	692 ewes	543 ewes		
SNP chip	MD	LD	MD	LD (n = 2,956)
	(n=3,225)	(n = 2,956)	(n = 664)	MD (n =3,889)
Genotyping age	>12 months	~15 days	8-12 months	

443 MD: medium density (50k), LD: low density (15k)

444 **Genotype quality control, imputation and phasing**

445 Quality control for each SNP was carried out following the French genomic evaluation pipeline
446 based on (i) call frequency >97%, (ii) minor allele frequency >1%, (iii) respect Hardy-Weinberg
447 equilibrium ($P > 10^{-5}$). Genotypes were phased and imputed from LD to MD using *FImpute3*
448 [67]. The accuracy of LD to MD imputation in MTR was previously assessed and resulted in a
449 concordance rate per animal of 98.86%, a concordance rate per SNP of 98.95% and a squared
450 Pearson's correlation coefficient of 93.57% between imputed and observed SNP genotypes
451 [68]. After quality control, the 38,523 remaining autosomal SNPs were mapped onto the *Ovis*

452 *aries* genome assembly Oar v3.1 (current version used in the French genomic evaluation) [69].
453 These SNP were also located on the genome assembly Oar_rambouillet_v1.0
454 (GCF_002742125.1). Genomic coordinates of both version of the sheep genome are available
455 at <https://doi.org/10.6084/m9.figshare.8424935.v2> (<https://www.sheepmap.org/>).

456 **Detection of homozygous haplotype deficiency**

457 Following the method used previously to detect deficit in homozygous haplotypes in sheep [42],
458 we screened the genome of the 5,271 genotyped animals belonging to trios (77 offspring had
459 both parents genotyped, and 4,799 offspring had both sire and maternal grandsire genotyped).
460 Briefly, the method consists in (i) screening the genome using a sliding window of 20 SNP
461 markers, (ii) selecting all 20 SNP haplotypes with frequency >1% on maternal phase, (iii)
462 comparing the observed number $N_{Obs}(k)$ to the expected number $N_{Exp}(k)$ of homozygous
463 offspring for each haplotype k using within-trios transmission probability and further
464 considered haplotypes with $P\text{-poisson} < 1.9 \times 10^{-4}$, (iv) retaining deficit between 75% and 100%
465 defined as $(N_{Exp}(k) - N_{Obs}(k)) / N_{Exp}(k)$. Finally, consecutive windows with these same
466 parameters were clustered to define larger region called “Manech Tête Rousse Deficient
467 Homozygous Haplotype” (MTRDHH). For each MTRDHH, the status (homozygous non-
468 carriers, heterozygous and homozygous carriers) was thereafter determined for all 6,845
469 genotyped animals available. Linkage disequilibrium was estimated between two MTRDHH
470 regions located on the same chromosome by the r^2 coefficient measure as described [42].

471 **Analysis of fertility traits**

472 Mating trait records of MTR between 2006 and 2019 were obtained from the national database
473 SIEOL. Only artificial insemination success (AIS) and stillbirth rate (SBR) records from mating
474 where both sire and maternal grand sire were genotyped (i.e. had a known status at each

475 MTRDHH) were analyzed. AIS was coded “1” for success and “0” for failure based on lambing
476 date according to the gestation length starting from the day of AI (151 ± 7 days; $n=330,844$
477 mating records). SBR was determined only in the AI success group, and coded “1” if there was
478 at least one stillbirth in the litter or “0” if all lambs were born alive ($n=201,637$ mating records).
479 We considered “at-risk mating” a mating between a carrier ram and a ewe from a carrier sire.
480 We considered “safe mating” when the other combinations occurred: (i) non-carrier ram \times ewe
481 from a non-carrier sire, (ii) non-carrier ram \times ewe from a carrier sire, (iii) carrier ram \times ewe
482 from a non-carrier sire. A logistic threshold binary model with a logit link function was used to
483 compare AIS and SBR between at-risk and safe mating (lsmeans estimate), using the
484 GLIMMIX procedure in the SAS software (version 9.4; SAS Institute Inc., Cary, NC). The
485 fixed effects for AIS and SBR were mating type (safe or at-risk), season of AI (spring or
486 summer), and lactation number (L1, L2, L3 and L4+). For SBR only, prolificacy of the ewe (1,
487 2, 3+ lambs/litter) was added as a fixed effect. For AIS and SBR, the random effect was the
488 interaction herd \times year ($n=313$ herds between 2006 and 2019). Traits were considered to differ
489 significantly when the mating type fixed effect had a P-value lower than 1.0×10^{-2} after
490 Bonferroni correction for multiple testing with a level of significance α at 5%. This threshold
491 was obtained by dividing the level of significance α by the number of tests corresponding to the
492 number of independent haplotypes ($n=5$).

493 **Analysis of milk parameters and total merit genomic index (ISOLg)**

494 Daughter yield deviations (DYD) for milk traits from genotyped sires with known status
495 at each MTRDHH were computed from official genetic evaluation (GenEval, Jouy-en-Josas,
496 France). The DYD corresponds to the average performance of the daughters of each sire,
497 corrected for environmental effects and the average genetic value of the dam [66]. The six traits
498 studied were milk yield (MY), fat (FC) and protein (PC) contents, fat (FY = MY \times FC) and

499 protein ($PY = MY \times PC$) yields, and lactation somatic cell score (LSCS) as described [42]. To
500 compare all the traits on the same scale, each DYD was divided by its genetic standard deviation
501 to obtain standardized DYD (sDYD). Only genotyped rams with records from at least 20
502 daughters were included in the analysis in order to obtain sufficiently accurate DYD values (n
503 ~2570 rams). Each trait was tested by variance analysis comparing MTRDHH carrier and non-
504 carrier rams using the GLM procedure in the SAS software (version 9.4; SAS Institute Inc.,
505 Cary, NC). The fixed effects were the genetic status (carrier, non-carrier) and year of birth
506 (2000 to 2016) to correct for annual genetic gain. Traits were considered to differ significantly
507 when the genetic status fixed effect had a P-value lower than 1.0×10^{-2} after Bonferroni
508 correction for multiple testing with a level of significance α at 5%. This threshold was obtained
509 as explained above for fertility traits (n=5 independent haplotypes).

510 Total merit genomic index in dairy sheep (called “ISOLg”, *Index Synthétique des Ovins*
511 *Laitiers*) was extracted from the official genomic evaluation (GenEval, Jouy-en-Josas, France)
512 for all the 714 genomic candidate lambs born in 2021. ISOLg is determined by a combination
513 of four selected traits: MY, FC, PC and LSCS. For each MTRDHH, ISOLg from heterozygous
514 carrier and non-carrier lambs were compared with a Wilcoxon non-parametric test under the
515 null hypothesis with a risk of $\alpha=5\%$ using “wilcox.test” function in R software (version 4.1.3,
516 R Core Team, 2022).

517 **Identification of positional and functional candidate genes**

518 All annotated genes located in the MTRDHH region extended by 1 Mb from each side were
519 extracted from the ovine genome Oar_rambouillet_v1.0 (OAR1: NC_040252.1, OAR10:
520 NC_040261.1, OAR13: NC_040264.1 and OAR20: NC_040271.1) using CLC export
521 annotation function (QIAGEN CLC Main Workbench 7.9). Genes with a known knock-out
522 phenotype in mouse including mortality and aging (embryonic, prenatal, perinatal, neonatal,

523 postnatal, preweaning, premature death and decreased survival rate) or associated with
524 mammalian genetic disorders were sorted using “biomaRt” R package (version 2.52.0,
525 <https://doi.org/doi:10.18129/B9.bioc.biomaRt>) extracted from Mouse Genome Informatics
526 (MGI, <http://www.informatics.jax.org>), International Mouse Phenotyping Consortium (IMPC,
527 <https://www.mousephenotype.org>), Online Mendelian Inheritance in Man (OMIM,
528 <https://omim.org>) and Online Mendelian Inheritance in Animal (OMIA, <https://omia.org>)
529 databases (last accession on 27 May 2022). Relevant candidate genes were presented as a
530 heatmap using “pheatmap” R package (version 1.0.12).

531 **Whole genome sequencing data**

532 Publicly available data of 100 ovine short-read Illumina HiSeq/NovaSeq whole genome
533 sequences (WGS) from 14 breeds generated in various INRAE and Teagasc research projects
534 were used for variant calling. Among them, 22 WGS were obtained from MTR dairy sheep also
535 genotyped with the MD SNP chip. A description of the different breeds and the accession
536 numbers of sequencing raw data are available in S3 Table.

537 **WGS variant calling and filtering**

538 Reads mapping, variant calling and functional annotation were performed using Nextflow
539 v20.10.0 and Sarek v2.6.1 pipelines for the 100 short-read WGS as previously described [43].
540 Regions of interest were extracted using SnpSift Filter, part of the SnpEff toolbox [51].
541 Candidate variants were filtered based on the correlation between haplotype status
542 (homozygous non-carriers, heterozygous and homozygous carriers encoded as 0, 1 and 2,
543 respectively) and allele dosage for bi-allelic variants (also encoded 0, 1 and 2) using `geno--r2`
544 command of VCFtools [70].

545 **Specific variant genotyping assays**

546 Genotyping at the *RXFP2* (1.8 kb InDel) and *ASIP* (5pb InDel) loci were directly
547 obtained from the LD SNP chip based on the specific markers described in S4 Table. The
548 NC_040264.1:g.66,474,980T>A in the last exon of *ASIP* and the SNP NC_040271.1:
549 g.23,776,347G>A in *MMUT* were both genotyped by PACE (PCR allele competitive extension)
550 analysis. Fluorescent PACE analysis was done with 15 ng of purified DNA using the PACE-
551 IR 2x Genotyping Master mix (3CR Bioscience) in the presence of 12 μ M of a mix of extended
552 allele specific forward primers and 30 μ M of common reverse primers in a final volume of 10
553 μ L (primer sequences described in S5 Table). The touch-down PCR amplification condition
554 was 15 min at 94°C for the hot-start activation, 10 cycles of 20 s at 94°C, 54–62°C for 60 s
555 (dropping 0.8°C per cycle), then 36 cycles of 20 s at 94°C and 60 s at 54°C performed on an
556 ABI9700 thermocycler followed by a final point read of the fluorescence on an ABI
557 QuantStudio 6 real-time PCR system and using the QuantStudio software 1.3 (Applied
558 Biosystems).

559 The presence of the *RXFP2*, *ASIP* and *MMUT* variants was checked in a DNA set of the
560 2021 cohort of 714 MTR male lamb candidates for genomic selection. DNA was extracted by
561 Labogena (Jouy-en-Josas, France) on behalf of the MTR breed industry. A DNA diversity panel
562 of 851 animals from 25 French sheep breeds [71] and 3 Spanish sheep breeds was also
563 specifically genotyped for the *MMUT* variant.

564 **Generation of homozygous lambs**

565 Blood samples (3 ml) were first collected from 181 ewes, daughters of MTRDHH1
566 carrier sires, located in 6 private farms by jugular vein puncture with the Venoject system
567 containing EDTA (Terumo, Tokyo, Japan) and directly stored at -20°C. Among them, 82 ewes

568 were genotyped as heterozygous carriers of the *MMUT* variant and were selected to be
569 inseminated with *MMUT* variant heterozygous rams (at-risk matings). Experiment 1 (n=73
570 ewes) was performed in 6 private farms in Pays-Basque (France) and Experiment 2 (n=9 ewes)
571 was performed at the INRAE experimental farm of Langlade under the agreement number
572 E31429001 (Pompertuzat, France). Experimental design is described in Fig 13. An ultrasound
573 diagnosis of gestation was realized between 45 and 60 days after AI. Gestations were followed
574 and each lamb was monitored from birth to weaning. Ear biopsies (1 mm³) from the 72 lambs
575 born in both experiments were obtained with a tissue sampling unit (TSU, Allflex Europe, Vitré,
576 France) and directly placed in the TSU storage buffer at 4°C. Ear biopsies were placed twice
577 consecutively in 180 µL of 50 mM NaOH, heated 10 min at 95°C, neutralized with 20 µL of 1
578 M Tris-HCl, and then vortexed during 10s. All neutralized samples were used for direct
579 genotyping without DNA purification as described [72]. In Experiment 2, all lambs were
580 weighted at birth. Biological samples (plasma, urine, liver and kidney) were collected on
581 animals as described in Fig 13 and frozen at -80°C until use.

582 **Immunoblot analysis**

583 Frozen kidney and liver tissues were crushed in liquid nitrogen using a Mixer Mill during 30
584 seconds at 30 Hz (MM400, Retsch technology), and 12 mg of tissue powder were lysed with
585 500µL of RIPA solution (Ref#R0278, Sigma-Aldrich). The protein extracts were centrifuged
586 for 20 minutes at 16 000g and 4°C, and protein concentration in the supernatant was determined
587 using BCA protein assay Kit (Ref#K812-1000, Biovision). Each protein sample (45 µg) was
588 denatured and reduced in Laemmli buffer (62.5mM TRIS pH 6.8, 2% SDS; 10% glycerol)
589 containing 5% β-mercaptoethanol before SDS-PAGE on a 4-15% polyacrylamide gel (Bio-
590 Rad). Proteins were transferred onto a nitrocellulose membrane blocked with AdvanBlock-
591 Chemi blocking solution (Advansta) during 1 hour at room temperature. After washing in PBS-

592 0.1% Tween 20, the membrane was incubated overnight à 4°C with a rabbit polyclonal anti-
593 MMUT primary antibody (MUT Rabbit pAb, Ref#A3969, ABclonal), followed (after washing)
594 by 1h with a rabbit polyclonal anti-Actin primary antibody (Ref#A2066, Sigma-Aldrich) both
595 at 1/1000 in blocking solution. Revelation of the primary antibodies was performed by
596 incubation with goat anti-rabbit Horseradish peroxidase-conjugated secondary antibody
597 (Ref#A0545, Sigma-Aldrich) at 1/10000 ratio in blocking solution for 1 hour at room
598 temperature, followed by enhanced chemiluminescence detection (WesternBright Quantum
599 HRP substrate, Advansta) on a ChemiDoc Touch low-light camera (Bio-Rad) in automatic
600 mode.

601 **RNA extraction, reverse transcription and quantitative PCR**

602 Total RNA was extracted from 80 mg of frozen kidney (n=15) and liver tissue powders (n=15)
603 in 1mL Trizol reagent (Invitrogen, #Ref 15596-018) and isolated from Nucleospin® RNA II
604 kit (Macherey-Nagel, #Ref 740955.50) according to the manufacturer's protocol and including
605 DNaseI digestion treatment. The RNAs were quantified by spectrophotometry (NanoDrop®
606 ND-8000 spectrophotometer, ThermoFischer) and stored at -80°C. Reverse transcription was
607 carried out from 1µg of total RNA in solution with anchored oligo(dT) T22V (1µL at 10µM),
608 random oligo-dN9 (1µL at 10µM) and dNTPs (2µL at 10 mM) in a reaction volume of 10 µL.
609 This mixture was incubated at 65°C for 5 min in an ABI2700 thermocycler (Applied
610 Biosystems) then ramped down to 4°C. A second reaction mixture (8 µL/reaction) containing
611 the reaction buffer (5µL of First strand Buffer 5X, Invitrogen, France), DTT (Dithiothreitol,
612 1µL at 0.1M), Rnasine (1µL, 40 units/µL, Promega, France) and Superscript II reverse
613 transcriptase (1µL, 200 units/µL, Invitrogen, France) was added to the denatured RNA solution
614 (final volume reaction of 18µL) then incubated for 50 minutes at 42°C and placed for 15
615 minutes at 70°C. The complementary DNA (cDNA) solution obtained was directly diluted at

616 1:5 ratio and stored at -20°C. For each pair of primers, amplification efficiency was evaluated
617 by $E = e^{-1/\alpha}$ which α is the slope of a linear curve obtained from cDNA serial dilution (1:5 to
618 1:80) and corresponding Ct (cycle threshold) values. Quantitative PCR (qPCR) was performed
619 using 3µL of cDNA at 1:20 ratio, 5µL of SYBR Green real-time PCR Master Mix 2X (Applied
620 Biosystems) and 2µL of primers at 3µM in a total reaction volume of 10µL on qPCR was
621 realized on a QuantStudio 6 Flex Real-Time PCR system (ThermoFisher). Each sample was
622 tested in duplicate. RNA transcript abundance was quantified using the $\Delta\Delta Ct$ method corrected
623 by four reference genes (*GAPDH*, *YWHAZ*, *RPL19* and *SDHA*) and a calibrator sample. Primers
624 were design using Beacon Designer™ 8 (Premier Biosoft). The list of qPCR primer sequences,
625 amplification length and amplification efficiency used is available in S5 Table.

626 **Methylmalonic acid dosage assay**

627 Dosage of methylmalonic acid (MLA) was performed on 11 urine and 15 plasma samples
628 collected on lambs. MLA dosage was performed using Sheep Methylmalonic Acid Elisa kit
629 (MyBioSource, Ref# MBS7266308) following the manufacture's protocol starting with 100µL
630 of samples. The incubation phase with specific antibody was performed overnight at 4°C. The
631 optical density at 450 nm was determined on a GloMax®-Multi Detection System (Promega).

632 **Ethic statement**

633 The experimental procedures on animals were approved (approval numbers APAFIS#30615-
634 2021032318054889 v5) by the French Ministry of Teaching and Scientific Research and local
635 ethical committee C2EA-115 (Science and Animal Health) in accordance with the European
636 Union Directive 2010/63/EU on the protection of animals used for scientific purposes.

637 **Acknowledgments**

638 We are grateful to the genotoul bioinformatics platform Toulouse Occitanie (Bioinfo Genotoul,
639 <https://doi.org/10.15454/1.5572369328961167E12>) for providing help and/or computing
640 and/or storage resources. The authors acknowledge the breeding confederations CDEO (Centre
641 Départemental de l’Elevage Ovin) and CONFELAC (Confederación de Asociaciones de
642 Criadores de Ovino de Razas Latxa y Carranzana) for providing access to private genomic data
643 and/or biological samples. We thank also the breeders involved in the project and Soline
644 Szymczak for help with genotyping.

645 **Funding**

646 This research has received funding from the European Union’s Horizon 2020 research and
647 innovation program under the Grant Agreement No. 772787 (SMARTER) and PRESAGE
648 project (CASDAR n°20ART1532777, the responsibility of the French ministry of Agriculture
649 and Food cannot be engaged). MB was supported by a Ph.D. grant for the HOMLET program
650 co-funded by APIS-GENE and Région Occitanie.

651 **References**

- 652 1. Georges M, Charlier C, Hayes B. Harnessing genomic information for livestock
653 improvement. *Nature Reviews Genetics*. 2019;20: 135–156. doi:10.1038/s41576-018-
654 0082-2
- 655 2. Rupp R, Mucha S, Larroque H, McEwan J, Conington J. Genomic application in sheep
656 and goat breeding. *Animal Frontiers*. 2016;6: 39–44. doi:10.2527/af.2016-0006
- 657 3. Eggen A. The development and application of genomic selection as a new breeding
658 paradigm. *Animal Frontiers*. 2012;2: 10–15. doi:10.2527/af.2011-0027
- 659 4. Chamberlain AJ, Cheng HH, Giuffra E, Kuehn C, Tuggle CK, Zhou H. Editorial:
660 Functional Annotation of Animal Genomes. *Frontiers in Genetics*. 2021;12. Available:
661 <https://www.frontiersin.org/article/10.3389/fgene.2021.768626>

- 662 5. Pryce JE, Royal MD, Garnsworthy PC, Mao IL. Fertility in the high-producing dairy cow.
663 Livestock Production Science. 2004;86: 125–135. doi:10.1016/S0301-6226(03)00145-3
- 664 6. Berry DP, Wall E, Pryce JE. Genetics and genomics of reproductive performance in dairy
665 and beef cattle. *Animal*. 2014;8: 105–121. doi:10.1017/S1751731114000743
- 666 7. David I, Astruc JM, Lagriffoul G, Manfredi E, Robert-Granié C, Bodin L. Genetic
667 Correlation Between Female Fertility and Milk Yield in Lacaune Sheep. *Journal of Dairy*
668 *Science*. 2008;91: 4047–4052. doi:10.3168/jds.2008-1113
- 669 8. Capitan A, Michot P, Baur A, Saintilan R, Hozé C, Valour D, et al. Genetic tools to
670 improve reproduction traits in dairy cattle. *Reprod Fertil Dev*. 2015;27: 14–21.
671 doi:10.1071/RD14379
- 672 9. Duchesne A, Grohs C, Michot P, Bertaud M, Boichard D, Floriot S, et al. From
673 phenotype to the causal mutation: recessive defects. *INRAE Productions Animales*.
674 2016;29: 319–328. doi:10.20870/productions-animales.2016.29.5.3000
- 675 10. Charlier C, Coppieters W, Rollin F, Desmecht D, Agerholm JS, Cambisano N, et al.
676 Highly effective SNP-based association mapping and management of recessive defects in
677 livestock. *Nat Genet*. 2008;40: 449–454. doi:10.1038/ng.96
- 678 11. Lander ES, Botstein D. Homozygosity Mapping: A Way to Map Human Recessive Traits
679 with the DNA of Inbred Children. *Science*. 1987;236: 1567–1570.
680 doi:10.1126/science.2884728
- 681 12. VanRaden PM, Olson KM, Null DJ, Hutchison JL. Harmful recessive effects on fertility
682 detected by absence of homozygous haplotypes. *Journal of Dairy Science*. 2011;94:
683 6153–6161. doi:10.3168/jds.2011-4624
- 684 13. Fritz S, Capitan A, Djari A, Rodriguez SC, Barbat A, Baur A, et al. Detection of
685 Haplotypes Associated with Prenatal Death in Dairy Cattle and Identification of
686 Deleterious Mutations in GART, SHBG and SLC37A2. *PLOS ONE*. 2013;8: e65550.
687 doi:10.1371/journal.pone.0065550
- 688 14. Pausch H, Schwarzenbacher H, Burgstaller J, Flisikowski K, Wurmser C, Jansen S, et al.
689 Homozygous haplotype deficiency reveals deleterious mutations compromising
690 reproductive and rearing success in cattle. *BMC Genomics*. 2015;16: 312.
691 doi:10.1186/s12864-015-1483-7
- 692 15. Jenko J. Analysis of a large dataset reveals haplotypes carrying putatively recessive lethal
693 and semi-lethal alleles with pleiotropic effects on economically important traits in beef
694 cattle. 2019; 14.
- 695 16. Hoff JL, Decker JE, Schnabel RD, Taylor JF. Candidate lethal haplotypes and causal
696 mutations in Angus cattle. *BMC Genomics*. 2017;18: 799. doi:10.1186/s12864-017-4196-
697 2
- 698 17. Cooper TA, Wiggans GR, Null DJ, Hutchison JL, Cole JB. Genomic evaluation, breed
699 identification, and discovery of a haplotype affecting fertility for Ayrshire dairy cattle.
700 *Journal of Dairy Science*. 2014;97: 3878–3882. doi:10.3168/jds.2013-7427

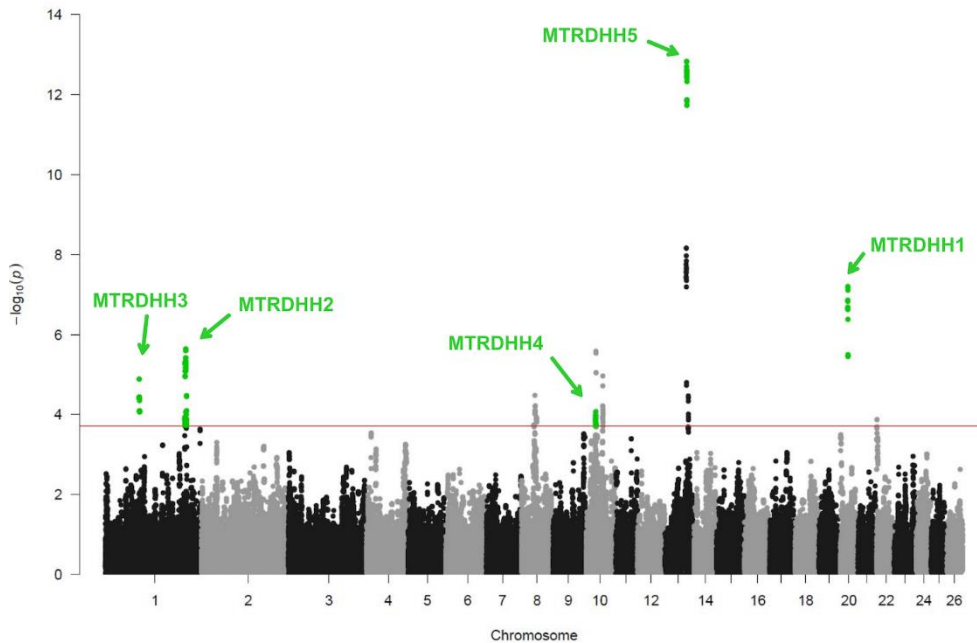
- 701 18. Null D, Hutchison J, Bickhart D, VanRaden P, Cole J. Discovery of a haplotype affecting
702 fertility in Ayrshire dairy cattle and identification of a putative causal variant. *Journal of*
703 *Dairy Science*. 2017;100(Suppl. 2): 199(abstr. 205).
- 704 19. Häfliger IM, Seefried FR, Spengeler M, Drögemüller C. Mining massive genomic data of
705 two Swiss Braunvieh cattle populations reveals six novel candidate variants that impair
706 reproductive success. *Genetics Selection Evolution*. 2021;53: 95. doi:10.1186/s12711-
707 021-00686-3
- 708 20. Sahana G, Nielsen US, Aamand GP, Lund MS, Guldbandsen B. Novel Harmful
709 Recessive Haplotypes Identified for Fertility Traits in Nordic Holstein Cattle. Pas MFW
710 te., editor. *PLoS ONE*. 2013;8: e82909. doi:10.1371/journal.pone.0082909
- 711 21. McClure MC, Bickhart D, Null D, VanRaden P, Xu L, Wiggans G, et al. Bovine Exome
712 Sequence Analysis and Targeted SNP Genotyping of Recessive Fertility Defects BH1,
713 HH2, and HH3 Reveal a Putative Causative Mutation in SMC2 for HH3. *PLOS ONE*.
714 2014;9: e92769. doi:10.1371/journal.pone.0092769
- 715 22. Cooper TA, Wiggans GR, VanRaden PM, Hutchison JL, Cole JB, Null DJ. Genomic
716 evaluation of Ayrshire dairy cattle and new haplotypes affecting fertility and stillbirth in
717 Holstein, Brown Swiss and Ayrshire breeds. 2013; ADSA-ASAS Joint Annual
718 Meeting :poster T206.
- 719 23. Fritz S, Hozé C, Rebours E, Barbat A, Bizard M, Chamberlain A, et al. An initiator codon
720 mutation in SDE2 causes recessive embryonic lethality in Holstein cattle. *Journal of Dairy*
721 *Science*. 2018;101: 6220–6231. doi:10.3168/jds.2017-14119
- 722 24. Hozé C, Fritz S, Baur A, Grohs C, Danchin-Burge C, Boichard D. Accounting for genetic
723 conditions in breeding objectives in dairy cattle. In *Proceedings of the 24ème Rencontres*
724 *Autour des Recherches Sur les Ruminants: 5-6 December. Paris; 2018.*
- 725 25. Häfliger IM, Spengeler M, Seefried FR, Drögemüller C. Four novel candidate causal
726 variants for deficient homozygous haplotypes in Holstein cattle. *Sci Rep*. 2022;12: 5435.
727 doi:10.1038/s41598-022-09403-6
- 728 26. Mesbah-Uddin M, Hozé C, Michot P, Barbat A, Lefebvre R, Boussaha M, et al. A
729 missense mutation (p.Tyr452Cys) in the CAD gene compromises reproductive success in
730 French Normande cattle. *Journal of Dairy Science*. 2019;102: 6340–6356.
731 doi:10.3168/jds.2018-16100
- 732 27. Häfliger IM, Seefried FR, Drögemüller C. Reverse Genetic Screen for Deleterious
733 Recessive Variants in the Local Simmental Cattle Population of Switzerland. *Animals*.
734 2021;11: 3535. doi:10.3390/ani11123535
- 735 28. Derks MFL, Megens H-J, Bosse M, Lopes MS, Harlizius B, Groenen MAM. A systematic
736 survey to identify lethal recessive variation in highly managed pig populations. *BMC*
737 *Genomics*. 2017;18: 858. doi:10.1186/s12864-017-4278-1
- 738 29. Derks MFL, Lopes MS, Bosse M, Madsen O, Dibbits B, Harlizius B, et al. Balancing
739 selection on a recessive lethal deletion with pleiotropic effects on two neighboring genes
740 in the porcine genome. Leeb T, editor. *PLoS Genet*. 2018;14: e1007661.
741 doi:10.1371/journal.pgen.1007661

- 742 30. Derks MFL, Megens H-J, Bosse M, Visscher J, Peeters K, Bink MCAM, et al. A survey
743 of functional genomic variation in domesticated chickens. *Genet Sel Evol.* 2018;50: 17.
744 doi:10.1186/s12711-018-0390-1
- 745 31. Abdalla EA, Id-Lahoucine S, Cánovas A, Casellas J, Schenkel FS, Wood BJ, et al.
746 Discovering lethal alleles across the turkey genome using a transmission ratio distortion
747 approach. *Animal Genetics.* 2020;51: 876–889. doi:10.1111/age.13003
- 748 32. Todd ET, Thomson PC, Hamilton NA, Ang RA, Lindgren G, Viklund Å, et al. A
749 genome-wide scan for candidate lethal variants in Thoroughbred horses. *Sci Rep.*
750 2020;10: 13153. doi:10.1038/s41598-020-68946-8
- 751 33. Venhoranta H, Pausch H, Flisikowski K, Wurmser C, Taponen J, Rautala H, et al. In
752 frame exon skipping in UBE3B is associated with developmental disorders and increased
753 mortality in cattle. *BMC Genomics.* 2014;15: 890. doi:10.1186/1471-2164-15-890
- 754 34. Schwarzenbacher H, Burgstaller J, Seefried FR, Wurmser C, Hilbe M, Jung S, et al. A
755 missense mutation in TUBD1 is associated with high juvenile mortality in Braunvieh and
756 Fleckvieh cattle. *BMC Genomics.* 2016;17: 400. doi:10.1186/s12864-016-2742-y
- 757 35. Burgstaller J, Url A, Pausch H, Schwarzenbacher H, Egerbacher M, Wittek T. Clinical
758 and biochemical signs in Fleckvieh cattle with genetically confirmed Fanconi-Bickel
759 syndrome (cattle homozygous for Fleckvieh haplotype 2). *Berl Munch Tierarztl*
760 *Wochenschr.* 2016;129: 132–137.
- 761 36. Adams HA, Sonstegard TS, VanRaden PM, Null DJ, Van Tassell CP, Larkin DM, et al.
762 Identification of a nonsense mutation in APAF1 that is likely causal for a decrease in
763 reproductive efficiency in Holstein dairy cattle. *Journal of Dairy Science.* 2016;99: 6693–
764 6701. doi:10.3168/jds.2015-10517
- 765 37. Yang Y, Si J, Lv X, Dai D, Liu L, Tang S, et al. Integrated analysis of whole genome and
766 transcriptome sequencing reveals a frameshift mutation associated with recessive
767 embryonic lethality in Holstein cattle. *Animal Genetics.* 2021;n/a. doi:10.1111/age.13160
- 768 38. Daetwyler HD, Capitan A, Pausch H, Stothard P, van Binsbergen R, Brøndum RF, et al.
769 Whole-genome sequencing of 234 bulls facilitates mapping of monogenic and complex
770 traits in cattle. *Nature Genetics.* 2014;46: 858–865. doi:10.1038/ng.3034
- 771 39. Schütz E, Wehrhahn C, Wanjek M, Bortfeld R, Wemheuer WE, Beck J, et al. The
772 Holstein Friesian Lethal Haplotype 5 (HH5) Results from a Complete Deletion of TBF1M
773 and Cholesterol Deficiency (CDH) from an ERV-(LTR) Insertion into the Coding Region
774 of APOB. *PLOS ONE.* 2016;11: e0154602. doi:10.1371/journal.pone.0154602
- 775 40. Michot P, Fritz S, Barbat A, Boussaha M, Deloche M-C, Grohs C, et al. A missense
776 mutation in PFAS (phosphoribosylformylglycinamide synthase) is likely causal for
777 embryonic lethality associated with the MH1 haplotype in Montbéliarde dairy cattle.
778 *Journal of Dairy Science.* 2017;100: 8176–8187. doi:10.3168/jds.2017-12579
- 779 41. Sonstegard TS, Cole JB, VanRaden PM, Van Tassell CP, Null DJ, Schroeder SG, et al.
780 Identification of a Nonsense Mutation in CWC15 Associated with Decreased
781 Reproductive Efficiency in Jersey Cattle. *PLOS ONE.* 2013;8: 54872.
782 doi:10.1371/journal.pone.0054872

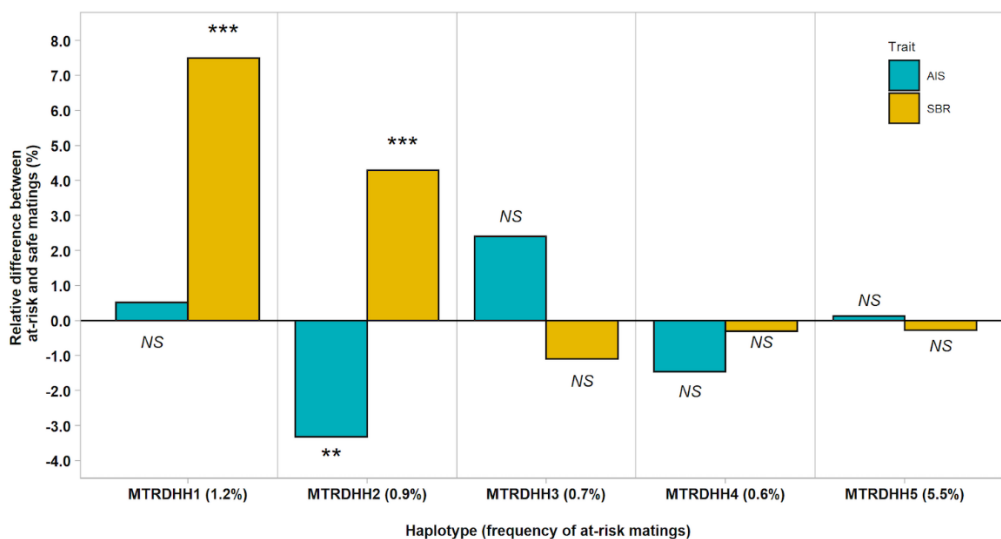
- 783 42. Ben Braiek M, Fabre S, Hozé C, Astruc J-M, Moreno-Romieux C. Identification of
784 homozygous haplotypes carrying putative recessive lethal mutations that compromise
785 fertility traits in French Lacaune dairy sheep. *Genetics Selection Evolution*. 2021;53: 41.
786 doi:10.1186/s12711-021-00634-1
- 787 43. Ben Braiek M, Moreno-Romieux C, Allain C, Bardou P, Bordes A, Debat F, et al. A
788 Nonsense Variant in CCDC65 Gene Causes Respiratory Failure Associated with
789 Increased Lamb Mortality in French Lacaune Dairy Sheep. *Genes*. 2022;13: 45.
790 doi:10.3390/genes13010045
- 791 44. Buisson D, Astruc J-M, Barillet F. Overview and perspectives of the management of
792 genetic diversity in French dairy sheep. *INRAE Productions Animales*. 2018;31: 1–12.
793 doi:10.20870/productions-animales.2018.31.1.2202
- 794 45. IDELE. VARUME. In: idele.fr [Internet]. 2016 [cited 14 Jun 2023]. Available:
795 [https://idele.fr/detail-article/indicateurs-de-variabilite-genetique-races-ovines-laitieres-](https://idele.fr/detail-article/indicateurs-de-variabilite-genetique-races-ovines-laitieres-edition-2016)
796 [edition-2016](https://idele.fr/detail-article/indicateurs-de-variabilite-genetique-races-ovines-laitieres-edition-2016)
- 797 46. Rodríguez-Ramilo ST, Elsen JM, Legarra A. Inbreeding and effective population size in
798 French dairy sheep: Comparison between genomic and pedigree estimates. *Journal of*
799 *Dairy Science*. 2019;102: 4227–4237. doi:10.3168/jds.2018-15405
- 800 47. Astruc J-M, Baloché G, Buisson D, Labatut J, Lagriffoul G, Larroque H, et al. Genomic
801 selection in French dairy sheep. *Inra Prod Anim*. 2016;29: 41–55.
- 802 48. Wiedemar N, Drögemüller C. A 1.8-kb insertion in the 3'-UTR of RXFP2 is associated
803 with polledness in sheep. *Animal Genetics*. 2015;46: 457–461.
804 doi:<https://doi.org/10.1111/age.12309>
- 805 49. Smit MA, Shay TL, Beever JE, Notter DR, Cockett NE. Identification of an agouti-like
806 locus in sheep. *Animal Genetics*. 2002;33: 383–385. doi:10.1046/j.1365-
807 2052.2002.00896_5.x
- 808 50. Norris BJ, Whan VA. A gene duplication affecting expression of the ovine ASIP gene is
809 responsible for white and black sheep. *Genome Res*. 2008;18: 1282–1293.
810 doi:10.1101/gr.072090.107
- 811 51. Cingolani P, Patel VM, Coon M, Nguyen T, Land SJ, Ruden DM, et al. Using *Drosophila*
812 *melanogaster* as a Model for Genotoxic Chemical Mutational Studies with a New
813 Program, SnpSift. *Frontiers in Genetics*. 2012;3: 35. doi:10.3389/fgene.2012.00035
- 814 52. Clark EL, Bush SJ, McCulloch MEB, Farquhar IL, Young R, Lefevre L, et al. A high
815 resolution atlas of gene expression in the domestic sheep (*Ovis aries*). *PLOS Genetics*.
816 2017;13: e1006997. doi:10.1371/journal.pgen.1006997
- 817 53. Derks MFL, Steensma M. Review: Balancing Selection for Deleterious Alleles in
818 Livestock. *Frontiers in Genetics*. 2021;12. Available:
819 <https://www.frontiersin.org/article/10.3389/fgene.2021.761728>
- 820 54. Beever JE, Smit MA, Meyers SN, Hadfield TS, Bottema C, Albretsen J, et al. A single-
821 base change in the tyrosine kinase II domain of ovine FGFR3 causes hereditary

- 822 chondrodysplasia in sheep. *Animal Genetics*. 2006;37: 66–71. doi:10.1111/j.1365-
823 2052.2005.01398.x
- 824 55. Boichard D, Grohs C, Danchin-Burge C, Capitan A. Genetic defects: definition, origin,
825 transmission and evolution, and mode of action. *INRAE Productions Animales*. 2016;29:
826 297–306. doi:10.20870/productions-animales.2016.29.5.2997
- 827 56. Lin P, Li J, Liu Q, Mao F, Li J, Qiu R, et al. A Missense Mutation in SLC33A1, which
828 Encodes the Acetyl-CoA Transporter, Causes Autosomal-Dominant Spastic Paraplegia
829 (SPG42). *The American Journal of Human Genetics*. 2008;83: 752–759.
830 doi:10.1016/j.ajhg.2008.11.003
- 831 57. Huppke P, Brendel C, Kalscheuer V, Korenke GC, Marquardt I, Freisinger P, et al.
832 Mutations in SLC33A1 Cause a Lethal Autosomal-Recessive Disorder with Congenital
833 Cataracts, Hearing Loss, and Low Serum Copper and Ceruloplasmin. *The American*
834 *Journal of Human Genetics*. 2012;90: 61–68. doi:10.1016/j.ajhg.2011.11.030
- 835 58. Acquaviva C, Benoist J-F, Pereira S, Callebaut I, Koskas T, Porquet D, et al. Molecular
836 basis of methylmalonyl-CoA mutase apoenzyme defect in 40 European patients affected
837 by mut^o and mut⁻ forms of methylmalonic acidemia: Identification of 29 novel mutations
838 in the MUT gene. *Human Mutation*. 2005;25: 167–176. doi:10.1002/humu.20128
- 839 59. Baumgartner MR, Hörster F, Dionisi-Vici C, Haliloglu G, Karall D, Chapman KA, et al.
840 Proposed guidelines for the diagnosis and management of methylmalonic and propionic
841 acidemia. *Orphanet J Rare Dis*. 2014;9: 130. doi:10.1186/s13023-014-0130-8
- 842 60. Deodato F, Boenzi S, Santorelli FM, Dionisi-Vici C. Methylmalonic and propionic
843 aciduria. *American Journal of Medical Genetics Part C: Seminars in Medical Genetics*.
844 2006;142C: 104–112. doi:10.1002/ajmg.c.30090
- 845 61. González-Montaña J-R, Escalera-Valente F, Alonso AJ, Lomillos JM, Robles R, Alonso
846 ME. Relationship between Vitamin B12 and Cobalt Metabolism in Domestic Ruminant:
847 An Update. *Animals*. 2020;10: 1855. doi:10.3390/ani10101855
- 848 62. Lucienne M, Aguilar-Pimentel JA, Amarie OV, Becker L, Calzada-Wack J, da Silva-
849 Buttkus P, et al. In-depth phenotyping reveals common and novel disease symptoms in a
850 hemizygous knock-in mouse model (Mut-ko/ki) of mut-type methylmalonic aciduria.
851 *Biochimica et Biophysica Acta (BBA) - Molecular Basis of Disease*. 2020;1866: 165622.
852 doi:10.1016/j.bbadis.2019.165622
- 853 63. Peters H, Nefedov M, Sarsero J, Pitt J, Fowler KJ, Gazeas S, et al. A Knock-out Mouse
854 Model for Methylmalonic Aciduria Resulting in Neonatal Lethality*. *Journal of*
855 *Biological Chemistry*. 2003;278: 52909–52913. doi:10.1074/jbc.M310533200
- 856 64. Charlier C, Li W, Harland C, Littlejohn M, Coppieters W, Creagh F, et al. NGS-based
857 reverse genetic screen for common embryonic lethal mutations compromising fertility in
858 livestock. *Genome Res*. 2016;26: 1333–1341. doi:10.1101/gr.207076.116
- 859 65. Legarra A, Baloche G, Barillet F, Astruc JM, Soulas C, Aguerre X, et al. Within- and
860 across-breed genomic predictions and genomic relationships for Western Pyrenees dairy
861 sheep breeds Latxa, Manech, and Basco-Béarnaise. *Journal of Dairy Science*. 2014;97:
862 3200–3212. doi:10.3168/jds.2013-7745

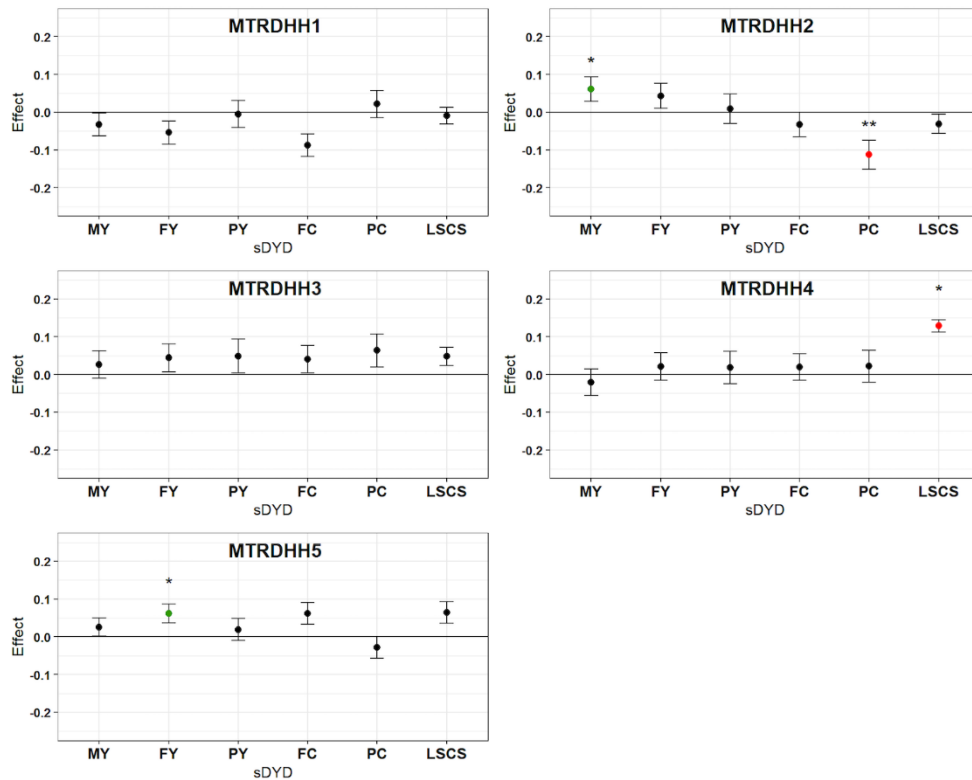
- 863 66. Astruc J-M, Baloché G, Buisson D, Labatut J, Lagriffoul G, Larroque H, et al. Genomic
864 selection in French dairy sheep. *Inra Prod Anim.* 2016;29: 41–55.
- 865 67. Sargolzaei M, Chesnais JP, Schenkel FS. A new approach for efficient genotype
866 imputation using information from relatives. *BMC Genomics.* 2014;15: 478.
867 doi:10.1186/1471-2164-15-478
- 868 68. Larroque H, Astruc J-M. Integration of a low density chip in dairy sheep genomic
869 selection. 2017 p. 27.
- 870 69. Jiang Y, Xie M, Chen W, Talbot R, Maddox JF, Faraut T, et al. The sheep genome
871 illuminates biology of the rumen and lipid metabolism. *Science.* 2014;344: 1168–1173.
872 doi:10.1126/science.1252806
- 873 70. Danecek P, Auton A, Abecasis G, Albers CA, Banks E, DePristo MA, et al. The variant
874 call format and VCFtools. *Bioinformatics.* 2011;27: 2156–2158.
875 doi:10.1093/bioinformatics/btr330
- 876 71. Rochus CM, Tortereau F, Plisson-Petit F, Restoux G, Moreno-Romieux C, Tosser-Klopp
877 G, et al. Revealing the selection history of adaptive loci using genome-wide scans for
878 selection: an example from domestic sheep. *BMC Genomics.* 2018;19: 71.
879 doi:10.1186/s12864-018-4447-x
- 880 72. Chantepie L, Bodin L, Sarry J, Woloszyn F, Plisson-Petit F, Ruesche J, et al. Genome-
881 Wide Identification of a Regulatory Mutation in BMP15 Controlling Prolificacy in Sheep.
882 *Front Genet.* 2020;11. doi:10.3389/fgene.2020.00585



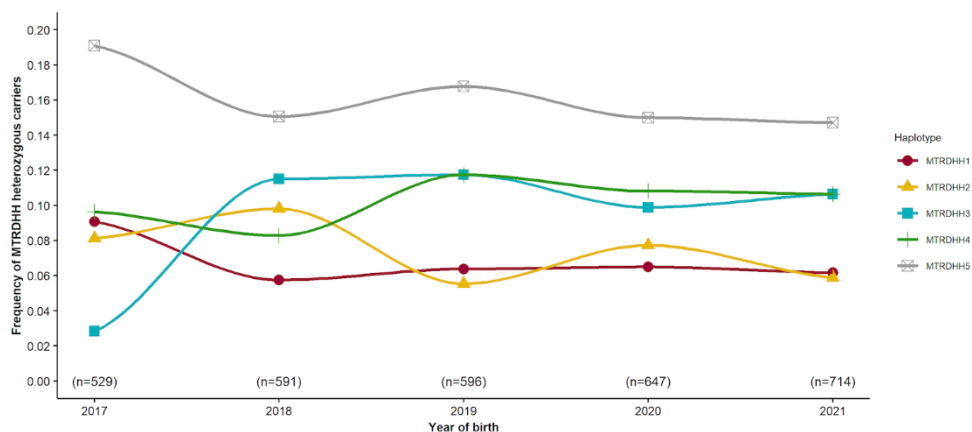
884 **Fig 1. Manhattan plot of HHD identified in Manech Tête Rousse dairy sheep.** Each point
 885 represents one haplotype of 20 markers with a frequency > 1% in the maternal phase. The red
 886 line represents the P-value threshold (1.9×10^{-4}) used to consider a haplotype with a significant
 887 deficit in homozygotes. Only HHD with a deficit in homozygotes $\geq 75\%$ (green dots) were
 888 selected and resulted in the identification of 150 significant HHD clustered in 5 regions
 889 (MTRDHH1 to 5). Genomic coordinates refer to the sheep reference genome Oar_v3.1.



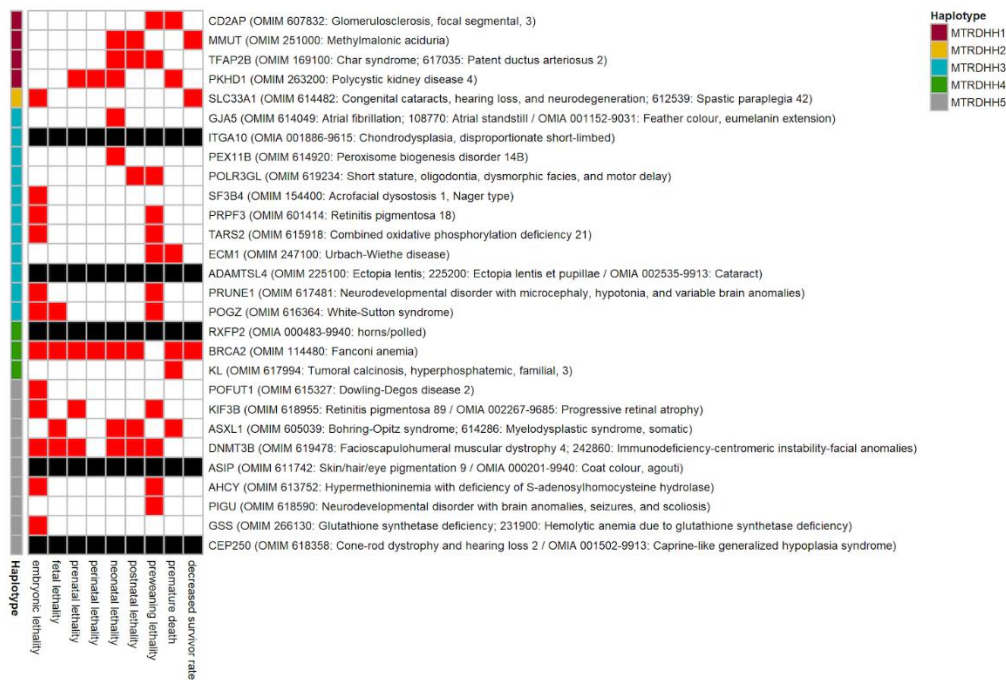
890 **Fig 2. Effects of MTRDHH on artificial insemination success (AIS) and stillbirth rate**
 891 **(SBR) between at-risk and safe matings.** For each MTRDHH, the frequency of at-risk
 892 matings is shown in parentheses. Significant effects are indicated by the corrected P-value for
 893 multiple tests with a threshold set at $\alpha=0.1\%$ (**), 0.01% (***) . NS, not significant.



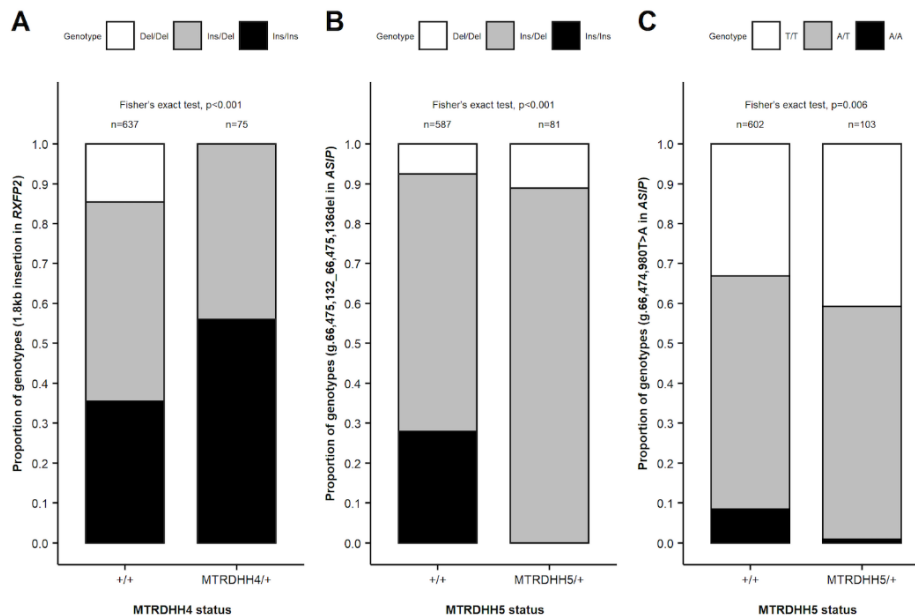
894 **Fig 3. sDSD relative difference between heterozygous and non-carrier rams for 6 traits**
 895 **under selection.** MY: milk yield, FY: fat yield, PY: protein yield, FC: fat content, PC: protein
 896 content, LSCS: lactation somatic cell score, sDSD standardized daughter yield deviation (DYD
 897 divided by genetic standard deviation). sDSD relative difference value is obtained from
 898 lsmeans estimate according to mating class. Significant effects are indicated by the corrected
 899 P-value for multiple tests with a threshold set at $\alpha=5\%$ (*), 0.1% (**). Error bars indicate
 900 standard errors. Significant favorable effects of heterozygous are in green while significant
 901 unfavorable effects are in red.



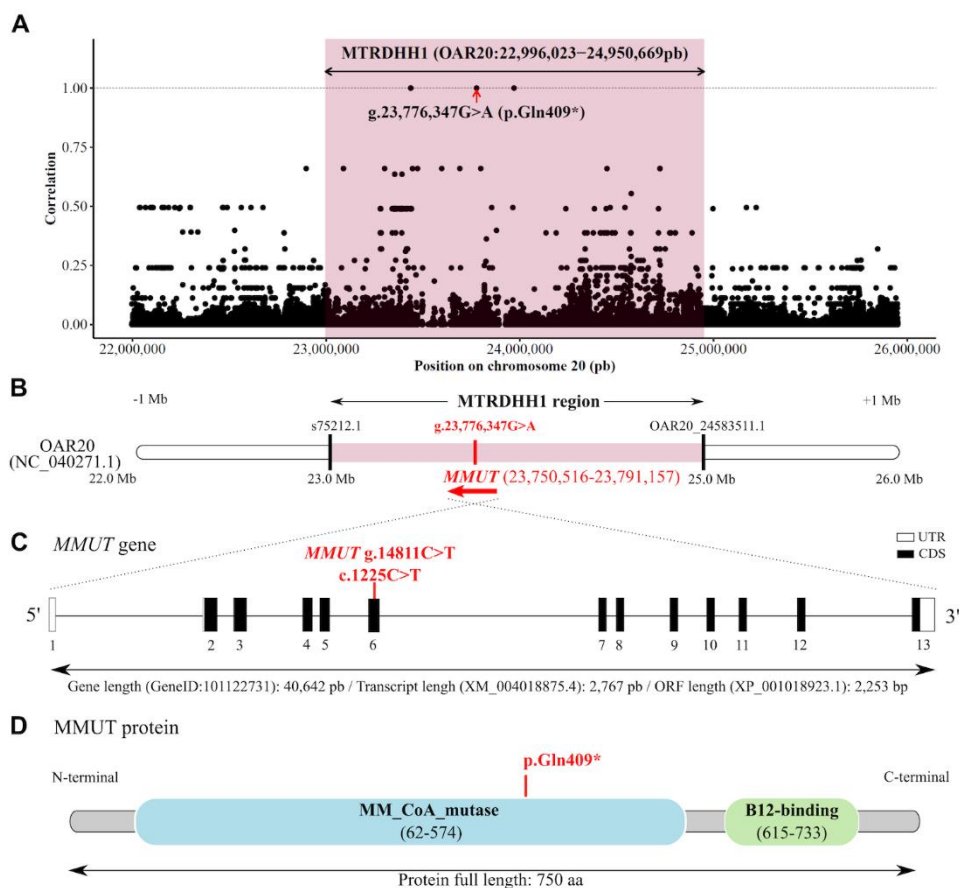
902 **Fig 4. Evolution of the MTRDHH heterozygous carrier frequencies between 2017 and**
 903 **2021 in Manech Tête Rousse male lambs.** For each year the effective refers to all candidates
 904 genotyped to enter in the genomic selection scheme.



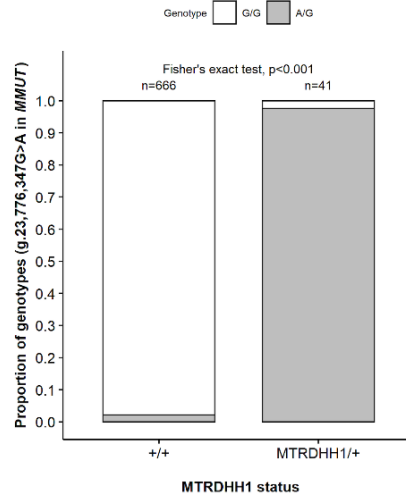
905 **Fig 5. Relevant candidate genes located in MTRDHH implicated in lethal mouse**
 906 **phenotype and/or associated with mammalian genetic disorders.** Red boxes indicate time
 907 of known lethality stages in mouse when the gene is knocked-out from MGI/IMPC databases.
 908 When the gene is associated with mammalian genetic disorders, the OMIM and/or OMIA trait
 909 phenotypes are described in parentheses. Black boxes indicate a gene implicated in animal
 910 genetic disorder (OMIA) but with no lethal phenotype observed in mouse.



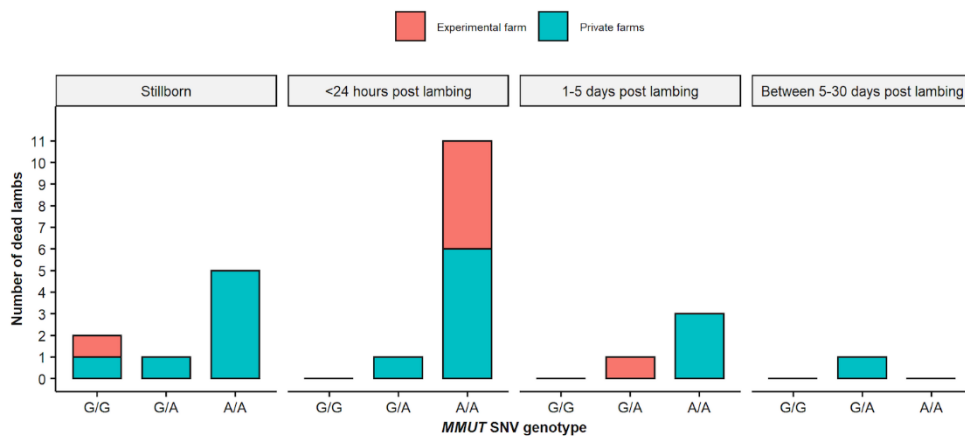
911 **Fig 6. Association between MTRDHH4-5 and causal variants involved in morphological**
 912 **traits.** (A) Association between MTRDHH4 status and 1.8kb insertion in the 3'-UTR of *RXFP2*
 913 associated with polledness. Association between MTRDHH5 status and (B)
 914 OAR13:g.66,475,132_66,475,136del and (C) OAR13:g.66,474,980T>A in *ASIP* associated
 915 with black coat color. Coordinates refer to sheep genome Oar_rambouillet_v1.0.



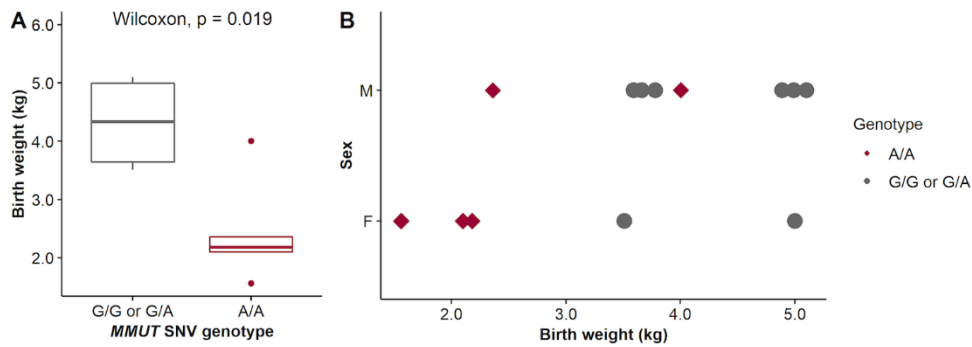
916 **Fig 7. Nonsense variant in *MMUT* gene within *MTRDHH1* genomic region.** (A) Scatter
 917 plot showing the correlation between *MTRDHH1* status (NC_040271.1, OAR20:22,996,023-
 918 24,950,669 extended from each side by 1 Mb) and genotype of variants from 100 whole genome
 919 sequenced animals. Each dot represents one variant. (B) Position of the *MMUT* gene within the
 920 *MTRDHH1* haplotype. Black bars indicate the first and the last markers of the Illumina Ovine
 921 SNP50 BeadChip defining the limits of *MTRDHH1* (S1B Table). (C) *MMUT* gene structure
 922 (GeneID: 101122731) and localization of the *MMUT* C>T polymorphism identified in the sixth
 923 exon (XM_004018875.4). (UTR: untranslated region; CDS: coding sequence) (D) *MMUT*
 924 protein (XP_004018923.1) with Pfam domain annotations (accession number:
 925 A0A6P3T7X3_SHEEP) composed of methylmalonyl-CoA mutase (PF01642) and B12-
 926 binding (PF02310) domains. The mutation creates a premature stop-gain at amino-acid position
 927 409.



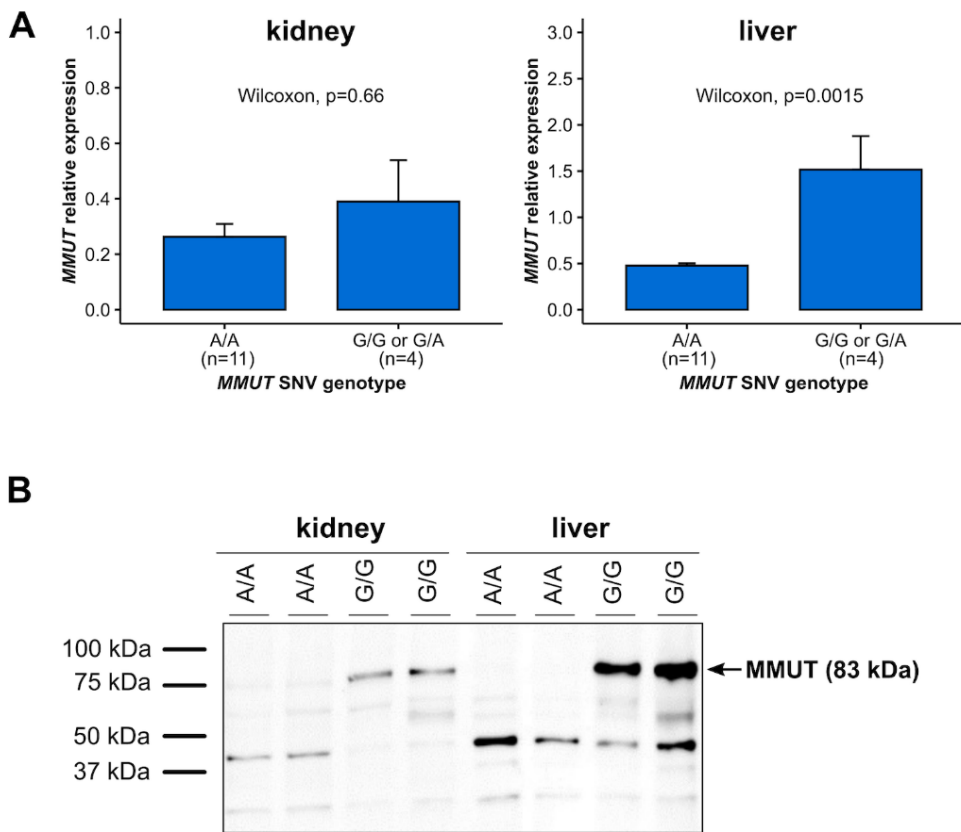
928 **Fig 8. Association of *MMUT* SNV genotypes with *MTRDHH1* status.** +/+ : non-carriers;
 929 *MTRDHH1* / + : heterozygous carriers and *MTRDHH1* / *MTRDHH1* : homozygous carriers
 930 (Fisher's exact test, $p < 0.001$, without the homozygous *MTRDHH1* carriers).



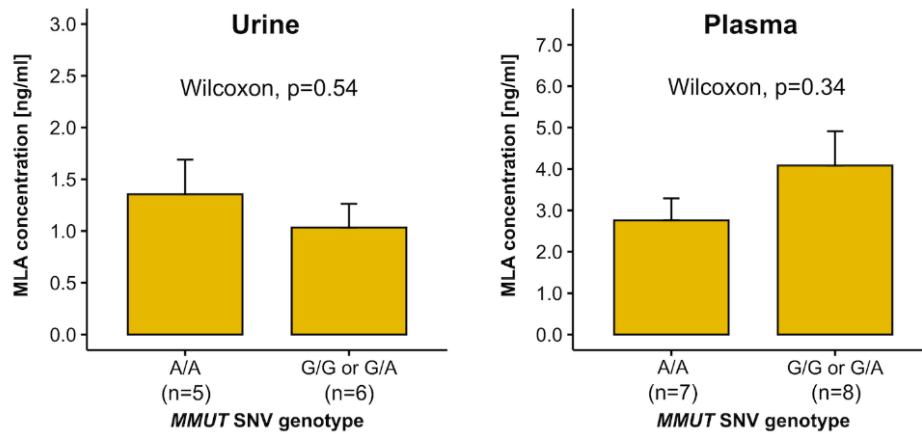
931 **Fig 9. Time distribution of dead lambs in the pre-weaning period.** Bar charts depending on
 932 *MMUT* SNV genotype and lambing place.



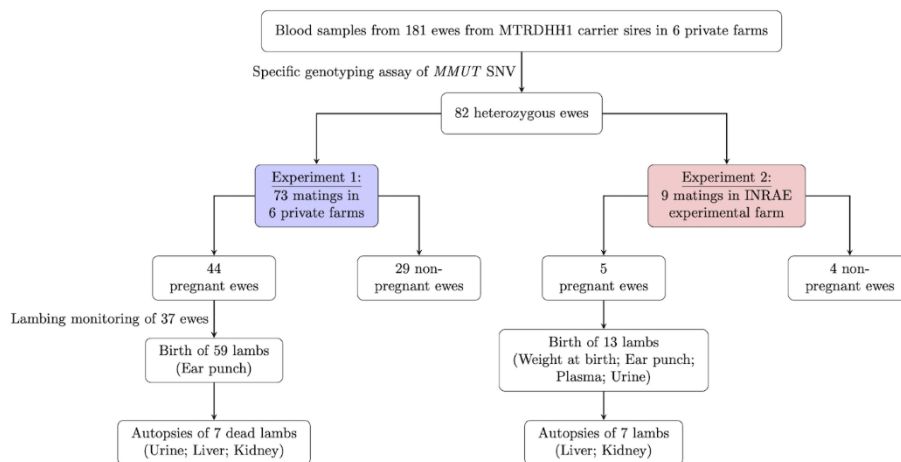
933 **Fig 10. *MMUT* SNV genotype effect on lamb birth weight.** (A) Boxplot representation of
 934 birth weight (n=13) according to *MMUT* genotypes (B) distribution of birth weight by sex (M:
 935 Male n=8, F: Female n=5) and genotypes. Affected homozygous lambs are in red (A/A
 936 genotype).



937 **Fig 11. RNA and protein expression of *MMUT* in homozygous A/A lambs.** *MMUT* gene
 938 expression (mean \pm SEM) at mRNA (A) and protein (B) levels in kidney and liver depending
 939 on *MMUT* SNV genotypes.



940 **Fig 12. Methylmalonic acid dosage in urine and plasma of A/A lambs.** Mean \pm SEM of
 941 Methylmalonic acid (MLA) ELISA quantification in blood plasma and urine collected from
 942 lambs of different genotypes at the *MMUT* SNV.



943 **Fig 13. Experimental design to generate *MMUT* homozygous variant lambs.**

944 Supporting information captions

945 **S1A Table. Clustering HHD into MTRDHH regions.** Table shows all significant haplotypes
946 of 20 markers (150 HHD with frequency > 1%, P-value < 1.9×10^{-4} and deficit $\geq 75\%$). As
947 described in the Materials and methods section, the 150 HHD could be clustered into 5
948 MTRDHH regions. **S1B Table. SNPs defining the MTRDHH regions.** Table gives the
949 position of each SNP within MTRDHH regions according to the sheep reference genomes
950 Oar_v3.1, Oar_rambouillet_v1.0 and ARS-UI_Ramb_v2.0, and the phased alleles of each
951 deficient haplotype.

952 **S1 Fig. Total merit genomic index (ISOLg) for the 2021 cohort genomic lambs (n=714).**
953 (A) Distribution of ISOLg in MTR dairy sheep. The ISOLg is determined by a combination of
954 four selected traits: MY, FC, PC and LSCS. Comparison of ISOLg according to each DHH
955 status, (B) MTRDHH1, (C) MTRDHH2, (D) MTRDHH3, (E) MTRDHH4, (F) MTRDHH5.

956 **S2 Table. List of the 408 protein coding genes located in the five MTRDHH extended by**
957 **1 Mb on each side.** Information on mouse phenotypes and association with mammalian
958 disorders were extracted for each gene using several databases: MGI: www.informatics.jax.org;
959 IMPC: <https://www.mousephenotype.org>); OMIM: Online Mendelian Inheritance in Man
960 (<https://omim.org>) and OMIA: Online Mendelian Inheritance in Animal (<https://omia.org>). For
961 mouse phenotypes associated with lethality, these were separated by developmental stages and
962 encoded 0 (no lethality) or 1 if the gene is involved in lethality at the given stage.

963 **S2 Fig. Association between MTRDHH4-5 and causal variants involved in morphological**
964 **traits from the 22 sequenced MTR animals.** (A) Association between MTRDHH4 status and
965 1.8kb insertion in the 3'-UTR of *RXFP2* associated with polledness. Association between
966 MTRDHH5 status and (B) OAR13:g.66,475,132_66,475,136del and (C)
967 OAR13:g.66,474,980T>A in *ASIP* associated with black coat color. Coordinates refer to sheep
968 genome Oar_rambouillet_v1.0.

969 **S3 Fig. MTRDHH1 recombinant haplotypes from 15 animals showing mismatch between**
970 **MTRDHH1 status and *MMUT* SNV genotype.** MTRDHH1/+ and +/+ refer to heterozygous
971 and non-carriers of MTRDHH1, respectively. The grey column represents the localization of
972 the *MMUT* SNV (g.23,776,347G>A) within the MTRDHH1 haplotype. For each animal, only
973 the phase supposed to host the *MMUT* SNV variant allele is represented. The blue color
974 indicates the portion of local haplotype matching with the MTRDHH1 haplotype.

975 **S4 Fig. Distribution of genotyped animals over time.** The bar charts represent the number of
976 genotyped animals according to sex and year of birth. The genomic selection in MTR dairy
977 sheep was implemented in 2017.

978 **S3 Table. EMBL-EBI accession numbers of the 100 whole-genome sequences used in the**
979 **analysis.**

980 **S4 Table. Markers on SheepLD chip for genotyping at the *RXFP2* (1.8 kb InDel) and *ASIP***
981 **(5pb InDel) loci.**

982 **S5 Table. List of PCR primer sequences.**